Drosophila Ge-1 is an essential P-body component involved in *oskar* mRNA localization

Shih-Jung Fan

August 2009

Dissertation

submitted to the

Combined Faculties for the Natural Sciences and for

Mathematics of the Ruperto-Carola University of

Heidelberg, Germany

for the degree of Doctor of Natural Sciences

presented by

Shih-Jung Fan (Diploma in Biology)

Born in Taipei, Taiwan

Oral Examination: October 07, 2009

Drosophila Ge-1 is an essential P-body component involved in *oskar* mRNA localization

Examiners: Prof. Dr. Matthias Hentze

Prof. Dr. Eduard Hurt

Contents

List of Figures

List of Tables

Abstract

Asymmetric localization of mRNAs is a highly conserved molecular mechanism to restrict protein expression that eukaryotic cells employ to achieve their polarized properties. In the *Drosophila* embryo, the posterior localization of Oskar protein, which instructs the development of the abdomen and pole cells in the embryo, is accomplished by first localizing *oskar (osk)* mRNA at the posterior pole of the oocyte. The localization of *osk* mRNA is mediated by trans-acting factors several of which have been shown to have roles in post-transcriptional regulation of RNA, such as splicing, translational control and degradation. However, most of the molecular mechanisms underlying *osk* mRNA localization are still unclear.

Recently, a new cellular structure, named processing body (P-body), was described as a repository for translationally quiescent mRNAs in eukaryotes. Several proteins involved in translation repression and degradation of mRNA are enriched in P-bodies. Although there is evidence showing that P-bodies are the sites where mRNA decay and translation repression can occur, the biological function of these structures remain elusive. Strikingly, several proteins that reside in P-bodies are also involved in *osk* mRNA localization and translational control, such as dDcp1 (*Drosophila* decapping protein 1), Cup, and Dhh/Me31B. Moreover, *in vivo,* the translation repressor Bruno provokes the formation of heavy *osk* mRNPs, aggregates containing multiple *osk* mRNA molecules in a translationally repressed state. The functional similarity between *osk* RNPs and P-bodies and the fact that they share some components suggest a close relationship between these two RNA-containing structures.

In order to get more insight into *osk* mRNA regulation, I focused on *Drosophila Ge-1*, *dGe-1*, whose mammalian homologue has been shown to be crucial for the formation of P-bodies in cells. During the course of this study, I have shown that dGe-1 protein localizes to P-bodies in the fly germline and associates with dDcp1, a P-body component. In addition, the formation of P-bodies is completely disrupted in *dGe-1* mutant egg-chambers, providing the first *in vivo* evidence that *dGe-1* is required for the P-body formation. Interestingly, some of the embryos derived from *dGe-1* mutant mothers exhibited posterior

patterning defects, suggesting a role of dGe-1 in *osk* mRNA regulation. Confirming this, examination of the distribution of *osk* mRNA in the oocyte revealed that its posterior localization is affected in the *dGe-1* mutant. Moreover, the *osk* mRNA mislocalization phenotype observed in the *dGe-1* mutant was enhanced by removal of a wild-type copy of the *osk* mRNP components Staufen (Stau), dDcp1 and Barentsz (Btz), suggesting that dGe-1 acts in conjunction with these three proteins in *osk* mRNA localization. Furthermore, immuno-electron microscopy revealed that dGe-1 is enriched on *osk* mRNA granules, suggesting that the effect of *dGe-1* on *osk* localization is direct. Taken together, the findings I have made have revealed the *in vivo* importance of dGe-1 protein in P-body assembly and in osk mRNA localization. The approach taken here also provides a new strategy for analyzing *osk* mRNA regulation through the study of key components of P-bodies or other types of RNA granules.

Zusammenfassung

Die asymmetrische Lokalisation von mRNA ist ein von eukaryotischen Zellen benutzter Mechanismus, um die Expression von Proteinen ganz gezielt und individuell zu regulieren und ermöglicht somit den Aufbau von interzellulären Polaritäten. Die posteriore Lokalisation von Oskar Protein - dem essentiellen Faktor für die Bildung der Keimbahnzellen und des Abdomens - im *Drosophila* Embryo ist entscheidend für die Entwicklung und wird weitgehend durch die Lokalisation des *oskar* Transkripts zum posterioren Pol erreicht. Am Transport der *oskar* mRNA sind viele Faktoren beteiligt, die auch an wichtigen post-transkriptionellen Prozessen wie der Kontrolle der Translation, der Degradation oder dem Spleißen des Transkripts beteiligt sind. Der genaue Mechanismus ist allerdings nach wie vor nicht verstanden.

Eine erst kürzlich beschriebene zelluläre Struktur, die Processing bodies (P-body), wurden als Depot für translationell inaktive mRNAs charakterisiert. In P-bodies sind zahlreiche Proteine engereichert welche bekannte Funktionen in der Translationskontrolle und der mRNA Degradation haben. Obwohl es Hinweise gibt, dass sowohl Repression als auch Degradation von mRNAs in P-bodies stattfindet, ist die genaue biologische Funktion noch unbekannt. Bemerkenswerterweise sind die P-body Komponenten dDcp1 (*Drosophila* decapping protein 1), Cup, und Dhh/Me31B auch in die Regulation der *oskar* mRNA involviert. Außerdem zeigten *in vivo* Experimente, dass der translationelle Repressor Bruno die Bildung von großen *oskar* mRNPs induzieren kann, die zahlreiche translationell repremierte *oskar* mRNAs enthalten. Diese Parallelität zwischen *oskar* RNPs and P-bodies, könnte auf eine enge Verwandtschaft dieser zwei Strukturen hindeuten.

Im Focus der vorliegenden Arbeit steht das Protein *Drosophila Ge-1*(*dGe-1*). Es wurde bereits gezeigt, dass sein Säugetier Homolog essentiell für die Bildung von P-bodies ist. Ich konnte zeigen, dass das dGe-1 Protein mit der P-body Komponente dDcp1 assoziiert und mit P-bodies der *Drosophila* Keimbahn colokalisiert. Außerdem zeigten dGe-1 mutante Eikammern eine vollständige Inhibition der Bildung von P-bodies. Dies ist der erste *in vivo* Hinweis dass dGe-1 essentiel für die Bildung von P-bodies ist. Außerdem zeigten Embryos von dGe-1 mutanten Müttern Defekte bei der Entwicklung posteriorer Strukturen, die auf Defizite in der *oskar* mRNA Lokalisation zurückzuführen waren. Dieser Effekt konnte durch die Entfernung einer Kopie der *oskar* RNP Komponenten Staufen (Stau), dDcp1 und Barentsz (Btz) verstärkt werden, was auf ein Zusammenwirken dieser Proteine mit dGe-1 hindeutet.

Mit immun-Elektronenmikroskopie konnte außerdem gezeigt werden, dass dGe-1 in *oskar* mRNA Partikeln angereichert ist, was den Schluss nahelegt, dass der Einfluss von dGe-1 auf die *oskar* Lokalisation direkt ist. Zusammenfassend konnte ich zeigen, dass dGe-1 essentiell für die *in vivo* Bildung von P-bodies und maßgeblich am *oskar* RNA Transport beteiligt ist. In dieser Arbeit konnte ich zeigen, dass dGe-1 *in vivo* essentiell für die Bildung von P-bodies ist und maßgeblich am *oskar* RNA Transport beteiligt ist. Außerdem lässt diese Beobachtung vermuten, dass P-body Komponenten an der post-transkriptionellen Kontrolle der *oskar* RNA beteiligt sind.

Abbreviations

A/P antero-posterior

BSA bovine serum albumin

bcd bicoid

btz barentzse

D/V dorso-ventral

EJC exon junction complex

EST expressed sequence tag

GFP green fluorescent protein

GLC germline clone

grk gurken

HA Human influenza hemagglutinin

hnRNP heterogenous ribonucleoprotein

khc Kinesin heavy chain

mRNP messenger ribonucleoprotein

NGS normal goat serum

osk oskar

PCR polymerase chain reaction

stau staufen

TSS transcription start site

UAS upstream activating sequence

UTR untranslated region

YFP yellow fluorescent protein

1. Introduction

1.1 mRNA localization

1.1.1 Various functions in different organisms

Asymmetric localization of mRNAs is now recognized as a powerful post-transcriptional mechanism to spatially and temporally regulate protein synthesis, thus allowing eukaryotic cells to achieve their polarized properties. mRNA localization has been shown to be involved in a variety of cellular processes in many organisms and many cell types. For example, the localization of *β-actin* mRNA at the leading edge in migratory chicken fibroblasts is required for their mobility (Figure 1A) (Condeelis et al., 2005). Similarly, in developing mouse neurons, the asymmetric distribution of *β-actin* mRNA in axonal growth cones is essential for directional turning during axon guidance (Figure 1B) (Lin and Holt, 2007; Yao et al., 2006). One of the best-studied examples is the localization of *ASH1* mRNA, which encodes a translation repressor of mating-type switching in the budding yeast. During cell division, *ASH1* mRNA is specifically targeted to the daughter cell and thereby restricts the protein only to the daughter cell nucleus. This ensures the distinctive cell fates of the mother and daughter cells after cell division (Figure 1D,E) (Long et al., 1997; Takizawa et al., 1997). mRNA localization also has been shown to play a crucial role in developmental processes. In the *Xenopus* oocyte, the mRNA of a T-box transcription factor VegT asymmetrically localizes to the vegetal pole and induces the endodermal and mesodermal cell fates in the future embryo (Figure 1C) (Zhang et al., 1998). Moreover, in *Drosophila*, *bicoid* (*bcd*) and *oskar* (*osk*) mRNA localize at the anterior and posterior cortex of the oocyte. Their localizations in the oocyte are crucial for the development of the anterior and posterior structures in the future embryo (Johnstone and Lasko, 2001).

Although only a few selected localized mRNAs have been studied in detail, recently numerous mRNAs have been found to be asymmetrically localized in cells. For example, a high-throughput *in situ* hybridization analysis of more than 3000 transcripts in *Drosophila* embryos showed that more than 70% of the transcripts are distributed in a spatially distinct manner and most of them

are localized into sub-cellular compartments (Lecuyer et al., 2007). Moreover, the identification of mRNAs from purified dendritic and/or synaptic compartments of neurons (Miyashiro et al., 1994; Moccia et al., 2004; Sung et al., 2004) have generated lists of localized mRNAs numbering in the hundreds . This suggests that mRNA localization is a more common biological phenomenon than previously thought.

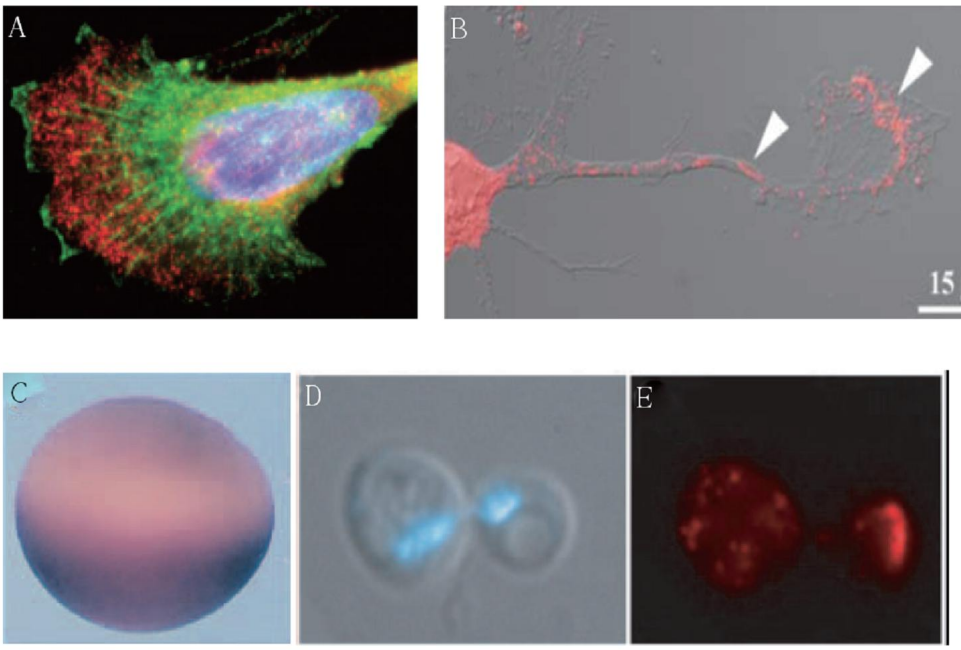

Figure 1 **Examples of mRNA localization in different organisms**
(A) *β-actin* mRNA (red) localizes to the leading edge of a migrating chicken fibroblast. Green: actin protein. Blue: the nucleus. (Image from Dahm and Kiebler, 2005) (B) In the developing neurites of a cultured mouse hippocampal neuron, *β-actin* mRNA (red) accumulates in the growth cone. Arrow heads: *β-actin* mRNA granules. (Image form Zhang et al., 2001) (C) *VegT* mRNA (dark blue) localizes to the vegetal hemisphere of the *Xenopus laevis* oocyte (image from Zhang and King, 1996) (D) A phase-contrast image of *Saccharomyces cerevisiae* shows a daughter cell (right) budding from the mother cell (left). Blue: the chromosomes. (Image from St Johnston, 2005) (E) *Ash1* mRNA (red) is localized to the tip of the daughter cell. (Image from St Johnston, 2005)

1.1.2 General mechanisms of mRNA localization

Eukaryotes have evolved different strategies to localize mRNAs into different subcellular compartments. One of these is to locally protect mRNAs from degradation. *hsp83* mRNA, encoding a component of the pole plasm in *Drosophila* embryos, is initially distributed evenly in the early stage embryo, but subsequently degraded throughout the entire embryo, except in the pole plasm, where the mRNA is protected (Ding et al., 1993). Another localization mechanism is by mRNA diffusion and trapping. An example of this is *nanos* mRNA, which passively diffuses throughout the oocyte during *Drosophila* oogenesis and gets specifically trapped in the posterior region of the oocyte (Forrest and Gavis, 2003).

The most commonly described mechanism of mRNA localization is active transport, by molecular motor proteins and the cytoskeleton. A general understanding of how active transport localizes mRNAs has developed from studies of a number of different mRNAs in various cell types. In general, it comprises four basic stages (Figure 2)(St Johnston, 2005). Firstly, in the nucleus, a nascent transcript whose localization signal is embedded in its sequence (often in its 3'UTR), associates with nuclear proteins to assemble an initial mRNP. Secondly, after being exported from the nucleus the mRNP matures further in the cytosol, for example, by recruitment of additional proteins that modify its composition. Thirdly, the matured mRNP is subsequently linked to motor proteins, via adaptor proteins, for its transport along the cytoskeleton. Finally, when the mRNA arrives at its target destination, it is anchored by proteins at that site to prevent its diffusion.

This four-step model of active mRNA transport is based on analysis of the transport of a single mRNA. However, it has been reported that transported mRNAs are found in larger structures, termed RNA transport granules. For example, in cultured oligodendrocytes, injected myelin basic protein (MBP) mRNAs assemble into granules that are transported through the dendritic processes to the periphery of the cell (Ainger et al., 1993). Moreover, the assembly of mRNAs into large complexes can also involve different mRNAs. In the budding yeast, simultaneous tracking of different localized mRNAs showed that they are co-assembled and co-transported for their localization in the daughter cell (Lange et al., 2008). These findings suggest that localizing mRNAs are transported in groups rather than individually. The assembly of

large RNA transport granules, whose function still remains elusive, adds one more layer of complexity to our current understanding of mRNA localization.

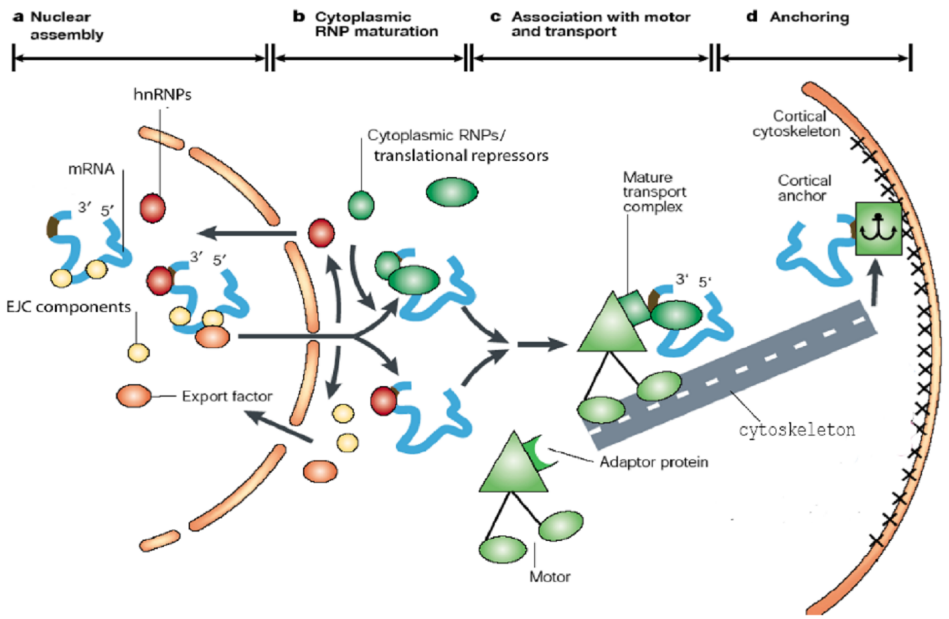

Figure 2 **A conceptual four-step model of active mRNA transport**

(A) In the nucleus the nascent transcript (blue) with its localization signal (brown) is associated with heterogeneous nuclear ribonucleoproteins (hnRNPs, red circles). Components of the exon junction complex (yellow circles) are deposited on the mature mRNA upon splicing. Export factors (orange ovals) also bind to the transcript. (B) Cytoplasmic proteins including translational repressors (green circles and ovals) associate with the exported transcript. Nuclear factors may dissociate from the transcript and recycle or remain bound to it. (C) Molecular motors (green triangles), through adaptor proteins, bind to the transport complex, which is then transported along the cytoskeleton to the target site. (D) When the transcript arrives at its final destination, it is anchored at the site. (adapted from St Johnston, 2005)

1.2 *Drosophila* oogenesis

The oocyte of *Drosophila melanogaster* has been a key model system for the analysis of mRNA localization, because of its large size and the availability of numerous genetic tools in this organism. Much of the detailed knowledge

about the mechanisms underlying mRNA localization has been gained through the investigation of three major localized mRNAs, *gurken* (*grk*), *bicoid* (*bcd*) and *oskar* (*osk*) in the *Drosophila* oocyte.

An adult *D. melanogaster* female has one pair of ovaries, each of which comprises16 to 20 ovarioles. Each ovariole contains a series of developing egg-chambers at different stages of maturation (Figure 3A, B). The ovariole can be divided into an anterior germarium and a posterior vitellarium (Figure 3C). At the tip of the germarium, germ stem cells divide asymmetrically to generate a new stem cell and a cystoblast. The cystoblast then undergoes four rounds of mitotic cell divisions with incomplete cytokinesis, resulting in a syncytium of 16 cells called a germline cyst (Huynh and St Johnston, 2004). Among these 16 cells, which are interconnected via the actin-rich ring canals, one of the two cells with four ring canals is selected to develop into an oocyte, while the other 15 cells differentiate into nurse cells. The germline cyst and the surrounding somatic follicular epithelial cells, which are derived from somatic stem cells in the germarium, give rise to a stage 1 egg-chamber (S1) that will mature gradually in the vitellarium. According to their morphology and size, egg-chamber development has been divided into 14 stages, S1 to S14 (King, 1970).

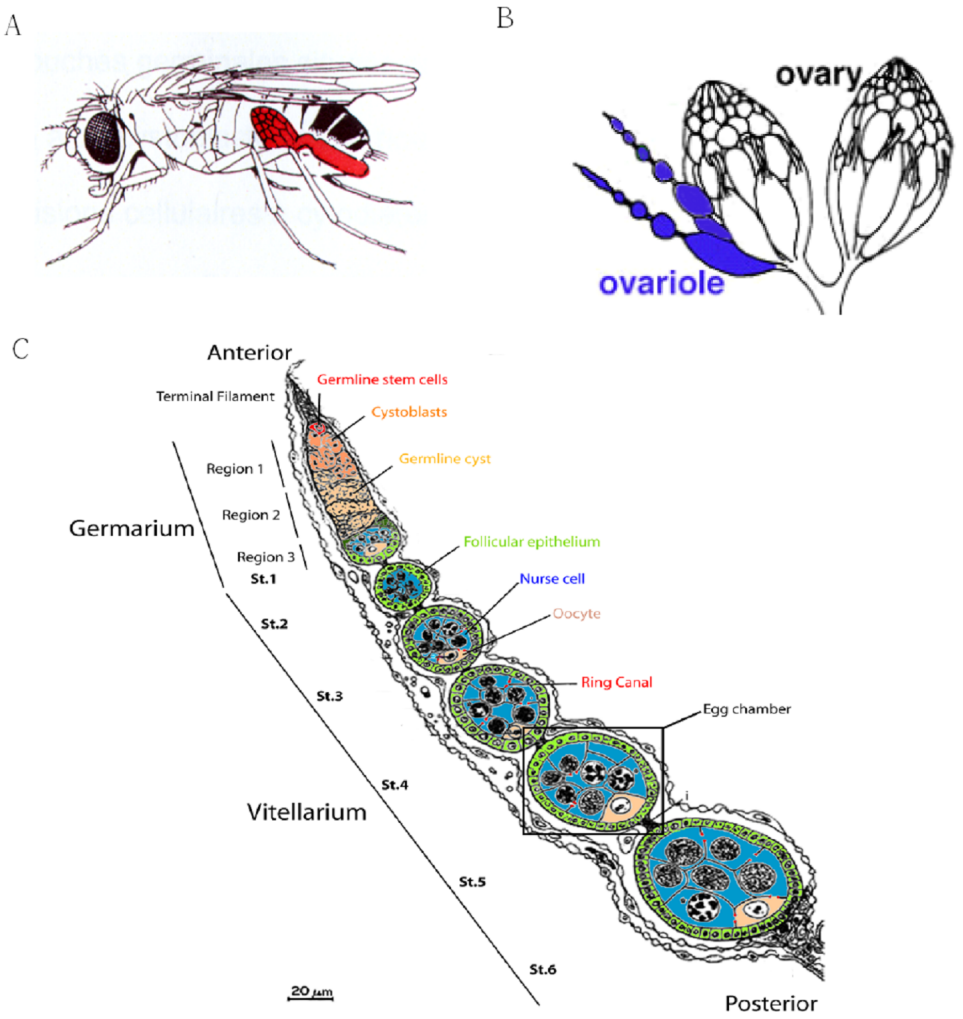

Figure 3 ***Drosophila* oogenesis**

(A) A schematic of an adult female fly. Its abdomen contains one pair of ovaries (red). (B) Diagram of the ovaries. One ovary comprises 16 to 20 ovarioles. Two ovarioles (blue) are are extruded from the ovary. (C) Illustration of one ovariole, which contains an anterior germarium and a posterior vitellarium. The germarium can be divided into three stages. The vitellarium contains the maturing egg-chambers, which can be divided into 14 stages. The first six stages of egg-chamber development are shown (adapted from King, 1970)

1.3 Axis determination of *Drosophila* embryo

The establishment of the body axes in the fly embryo initiates in the oocyte by the precise localization of three mRNAs *grk*, *bcd* and *osk* (Figure 4A, B, C). During oogenesis these three mRNAs are synthesized in the nurse cells, then transported into the oocyte, and finally localized in the antero-dorsal, anterior, and posterior regions of the oocyte, respectively (Riechmann and Ephrussi, 2001).

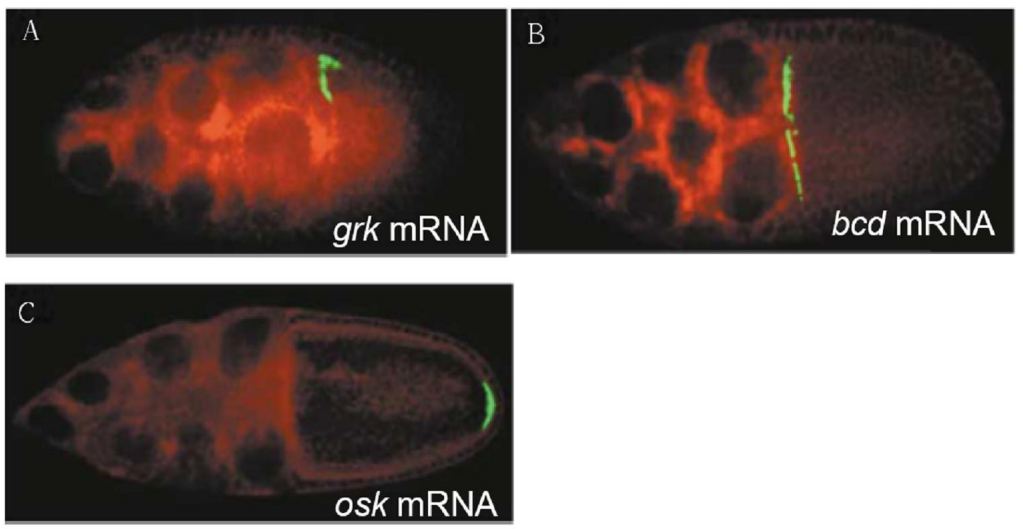

Figure 4 **Localization of *gurken*, *bicoid* and *oskar* mRNAs in the *wild-type* egg-chamber**

mRNAs are shown in green. (A) *gurken* mRNA is localized at the antero-dorsal corner of the oocyte in a S9 egg chamber. (B) *bicoid* mRNA is localized at the anterior cortex of the oocyte in a S10 egg chamber. (C) *oskar* mRNA is localized at the posterior pole of an S10 oocyte (image from Hachet and Ephrussi, 2001)

1.3.1 Determination of the dorso-ventral axis by *grk*

grk gene encodes a TGF-α-like protein involved in EGFR signaling in the fly. It was first identified by the distinctive ventralized "gurken-looking" embryonic phenotype that resulted from depleting *grk* in the oocyte (Schupbach, 1987). This study also revealed a critical role of maternal *grk* in determination of the

dorso-ventral (D/V) axis in the embryo. During S8 of oogenesis, *grk* mRNA accumulates at the antero-dorsal corner of the oocyte, in tight association with the oocyte nucleus (Neuman-Silberberg and Schupbach, 1993). This spatial restriction of *grk* mRNA constrains the distribution of its protein. Thus, the EGFR signaling is only activated in the adjacent follicle cells, which as a result acquire the dorsal cell fate, while the rest of the follicle cells adapt the ventral cell fate. The D/V polarization of the follicle cells sequentially instructs the polarization of the oocyte, which in turn determines the D/V axis of the resulting embryo (Schupbach, 1987).

1.3.2 Determination of the anterio-posterior axis by *bcd*

The establishment of the antero-posterior axis of the embryo depends on two mRNAs, *bcd* and *osk*, which are localized at the anterior and posterior poles of the oocyte, respectively.

From S7 to S9 of oogenesis, *bcd* mRNA is transcribed in nurse cells, where its expression is regulated by Serendioity δ (Payre et al., 1994), then transported into the oocyte in a microtubule-dependent manner (Cha et al., 2001), where it finally accumulates at the anterior cortex of the oocyte through a process involving Exuperantia protein (Riechmann and Ephrussi, 2004). *bcd* mRNA anchoring during late oogenesis and early embryogenesis depends on the double-stranded RNA binding protein Staufen (Stau) (Ephrussi and St Johnston, 2004).

Upon egg activation, which usually occurs at fertilization in *Drosophila*, *bcd* mRNA is translated, forming a concentration gradient with its highest level at the anterior end of the embryo. Bcd encodes a homeodomain-containing transcription and translation factor (Cho et al., 2005; Driever and Nusslein-Volhard, 1989). As a transcription factor, the Bcd protein directly regulates transcription of a dozen of genes, including the gap and pair-rule genes, along the A/P axis. As a translation repressor, it inhibits the translation of *caudal* mRNA, which is required for development of the posterior structures of the embryo (Cho et al., 2005; Mlodzik and Gehring, 1987). With its dual activities Bcd protein instructs formation of the head and thorax at the anterior of the embryo.

1.3.3 *osk*, a posterior determinant

The biological function of *osk* in development was brought to light by its mutant phenotype. The progeny of the weak *osk* mutants develop into sterile adults, resulting in a “grandchildless” phenotype (Lehmann and Frohnhofer, 1989). This sterility is due to the absence of pole cells, the primordial germ cells of the fly, which are among the posterior cell types that develop in the early embryo and are required for adult gonad development. This weak *osk* mutant phenotype was the first indication of a potential function of *osk* in the development of posterior structures in the embryo. The role of *osk* became much clearer after a strong *osk* mutant allele was identified. Embryos entirely depleted of maternal *osk* activity die during embryonic development and exhibit the so-called “posterior group” phenotype, recognized by the loss of posterior structures, including the pole cells and the abdomen (Figure 5A, B) (Ephrussi and Lehmann, 1992; Lehmann and Nusslein-Volhard, 1986). Moreover, ectopic expression of Osk protein can induce the ectopic formation of abdominal structures and pole cells at the anterior of the embryo (Figure 5C) (Figure 5C) (Ephrussi and Lehmann, 1992). Thus, Osk activity is both necessary and sufficient for posterior structure formation.

Osk protein is produced once *osk* mRNA reaches the posterior pole of the oocyte. Two Osk protein isoforms, Long Osk and Short Osk, are generated from *osk* mRNA using two different translational start codons (Markussen et al., 1995). Long Osk has been shown to be required for the anchoring of *osk* mRNA and Short Osk at the posterior pole (Vanzo and Ephrussi, 2002), whereas Short Osk nucleates the assembly of the polar granules, which instructs the development the pole cells (Markussen et al., 1995). In conclusion, the Long and Short Osk proteins, which are generated at the posterior of the oocyte, cooperate to induce the formation of the posterior structure of the embryo.

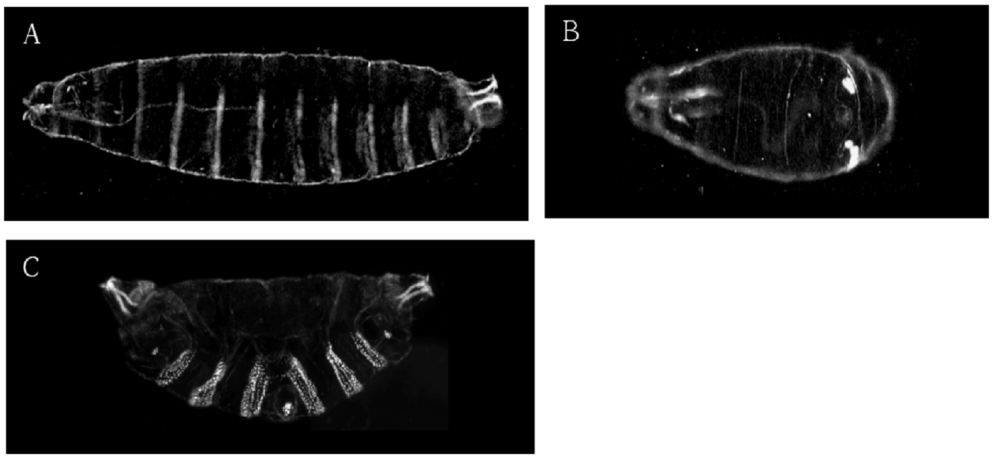

Figure 5 **Osk function in patterning of the *Drosophila* embryos**
A ventral view of *Drosophila melanogaster* embryos. Anterior: left. Posterior: right. (A) In the *wild-type* embryo, the eight abdominal denticle belts are clearly visible on the ventral side of the embryo. (B) However, in an *osk*⁻ mutant embryo, the absence of Osk protein causes the absence of the abdominal denticle belts, a prominent characteristic of abdominal deletion. (C) Strikingly, in embryos in which Osk protein is ectopically expressed at the anterior, posterior structures are duplicated at the anterior, where anterior structures, namely the head and thorax, would normally form. (Images from Ephrussi and Lehmann, 1992)

1.4 *osk* mRNA localization and translation repression during oogenesis

1.4.1 *osk* mRNA localization during early oogenesis

osk mRNA is transcribed in the nucleus of the nurse cells and is subsequently transported into the oocyte. Its distribution in the oocyte is very dynamic throughout oogenesis. During S2 to S6 , *osk* mRNA as well as other mRNAs, such as *grk,* are enriched in the oocyte (Figure 6A) (Cheung et al., 1992; Clark et al., 2007; Ephrussi et al., 1991; Kim-Ha et al., 1991). This enrichment depends on an intact microtubule network and the Bicaudal-D (Bic-D)/ Egalitarian (Egl) complex, which are thought to couple mRNA cargoes to the

motor dynein for transport towards the minus end of microtubules (Bullock and Ish-Horowicz, 2001; Clark et al., 2007; Pokrywka, 1995; Swan and Suter, 1996). Interestingly, at these stages the microtubules of the germline cyst have their minus ends in the oocyte and extend into the nurse cells though the ring canals. Based on this that it was proposed that a microtubule minus-end-directed transport mechanism underlies the oocyte enrichment of *osk* mRNA during early oogenesis.

1.4.2 *osk* mRNA localization during mid-oogenesis

During S7 to S8, concomitant with the reorganization of the microtubule network in the oocyte, *osk* mRNA accumulates transiently in the center, as well as at the anterior pole of the oocyte (Cha et al., 2002). After this reorganization, the microtubules form a gradient with their highest concentration at the anterior of the oocyte (Cha et al., 2002) and *osk* mRNA becomes localized to the posterior pole of the oocyte, where it persists until early embryogenesis (Figure 6B) (Ephrussi et al., 1991; Kim-Ha et al., 1991). This phase in the posterior translocation of *osk* mRNA has been widely used as an *in vivo* model to study mRNA localization.

1.4.2.1 Molecular mechanism of *osk* mRNA localization during mid-oogenesis

As with many other localized mRNAs, the localization signals in *osk* mRNA are embedded in its sequence (Jansen, 2001). Based on deletion analysis, the 3'UTR of *osk* mRNA was shown to be required for its posterior localization (Kim-Ha et al., 1993). In the 3'UTR, several cis-regulatory elements were shown to be involved in the different steps of *osk* mRNA localization, suggesting they might be recognized by different trans-acting factors coupling the mRNA with different transport machineries (Kim-Ha et al., 1993). Although the *osk* 3'UTR is essential for its localization, it is not sufficient. It was later shown that the presence of the first intron in *osk* is also required in a sequence-independent manner for localization of the mRNA, suggesting that splicing of the first intron of *osk* mRNA in the nucleus plays a crucial role in this process (Hachet and Ephrussi, 2004).

Consistent with the necessity for splicing in *osk* mRNA localization, the core

components of the Exon Junction Complex (EJC), which is deposited on mature mRNAs upon splicing (Le Hir et al., 2000; Tange et al., 2005), are also required (Hachet and Ephrussi, 2001; Mohr et al., 2001; Newmark and Boswell, 1994; Palacios et al., 2004; van Eeden et al., 2001). Mutations that affect any of the four core components, Y14, Mago nashi (Mago), Barentsz (Btz), and eIF4AIII, affect *osk* mRNA localization. In addition to the EJC core components, several other trans-acting factors required for the targeting of *osk* mRNA also act in the nucleus, where *osk* RNA is synthesized (St Johnston, 2005). Among these is Hrp48, which belongs to the hnRNP (heterogeneous nuclear ribonucleoprotein) A/B family (Dreyfuss et al., 2002). With its ability to bind both the 5' and 3' UTR of *osk* mRNA, Hrp48 associates with *osk* mRNA in the nucleus and persists on *osk* mRNA in the cytoplasm, where it is required for its posterior localization (Huynh et al., 2004; Yano et al., 2004) (A. Trucco, personal communication). Therefore, the formation and the fate of the *osk* mRNA localization complex depend on its nuclear history.

After UAP56-mediated export from the nucleus (Meignin and Davis, 2008), *osk* mRNA associates with its cytoplasmic partners. One of them is Staufen (Stau), a conserved protein featuring five dsRNA-binding motifs (St Johnston et al., 1991). In the oocyte Stau colocalizes with *osk* mRNA and is required for its localization (St Johnston et al., 1991). Another cytoplasmic component that functions in the posterior localization of *osk* mRNA is *Drosophila* decapping protein 1 (dDcp1) (Lin et al., 2006). In *dDcp1* mutant egg-chambers, *osk* mRNA frequently localizes to the anterior of the oocyte. However, the mechanism by which dDcp1 protein mediates *osk* mRNA localization to the posterior pole remains mysterious, since there is no evident relationship between its well-known role in mRNA degradation (Tucker and Parker, 2000) and a function in mRNA localization.

It has been shown that the transport of *osk* mRNA to the posterior pole is microtubule-dependent: posterior localization of *osk* mRNA is abolished in oocytes treated with the microtubule depolymerizing drug colchicine (Theurkauf et al., 1992). Moreover, the mutation of Kinesin heavy chain (Khc), a key component of the microtubules plus-end motor kinesin-1, leads to mislocalization of *osk* mRNA (Brendza et al., 2000a; Clark et al., 1994; Palacios and St Johnston, 2002). Also, a chimeric protein consisting of the Khc motor domain fused to beta-galactosidase colocalizes with *osk* mRNA (Clark et al., 1994). Thus, it has been suggested that after a proper *osk* mRNP has

been assembled, it associates with Kinesin for its transport along microtubules to the posterior pole of the oocyte. However, there is no biochemical evidence proving a direct interaction between the *osk* mRNP and Kinesin motor protein. Recent *in situ* EM data from our laboratory does show that all *osk* RNA particles in the oocyte are closely associated with Khc molecules, suggesting that they are indeed actively transported by kinesin-1 to the posterior pole (A. Trucco, personal communication).

1.4.2.2 Translation repression of *osk* mRNA

During its transport, *osk* mRNA translation must be repressed (Figure 6C, D), as ectopic production of Osk protein, which is sufficient for posterior structure formation, is deleterious for embryonic development (Ephrussi and Lehmann, 1992) (see section 1.3.3). As in the case of the RNA localization signals, the information for *osk* mRNA translation repression is also embedded in the RNA sequence. In the *osk* 3'UTR, the BREs (Bruno Response Elements), which are recognized by Bruno protein, are crucial for *osk* translation repression (Kim-Ha et al., 1995). Deletion of the BREs from an *osk* transgene leads to its premature translation, whereas insertion of BREs into a heterologous mRNA confers translation repression upon it (Kim-Ha et al., 1995). Cup, protein which directly associates with Bruno, is also involved in *osk* translation repression (Nakamura et al., 2004). Cup, a functional homologue of 4E-T (Ferraiuolo et al., 2005), can bind eIF-4E and compete with eIF-4G for eIF-4E binding, thus inhibiting translation (Nakamura et al., 2004). Me31B, the *Drosophila* homologue of Dhh1/p54/Rck, an RNA helicase involved in general translation repression and decapping processes in mRNA degradation (Coller et al., 2001; Minshall and Standart, 2004), is also required for *osk* translation repression (Nakamura et al., 2001). In the *Me31B* mutant, Osk protein is precociously made in the oocyte, as well as in the nurse cells in young egg chambers. However, the molecular mechanism of *Me31B* function in *osk* mRNA translation repression still needs to be addressed.

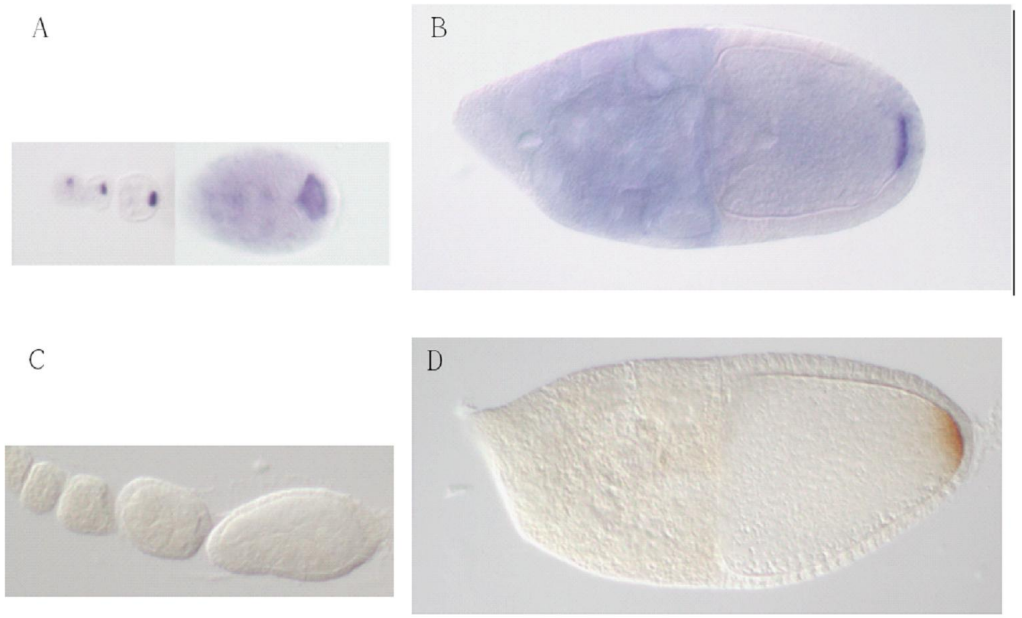

Figure 6 **The distribution of *osk* mRNA and its protein during oogenesis**
A, B) *osk* mRNA distribution revealed by *in situ* hybridization using an *osk* antisense RNA probe. (A) During early oogenesis, *osk* mRNA is enriched in the oocyte. (B) At mid-oogenesis, such as S10 shown here, *osk* mRNA is localized at the posterior pole of the oocyte. (C, D) Osk protein is detected by immuno-histochemical staining using an anti-Osk antibody. (C) During early oogeneis, Osk protein is not detected in the oocyte or the nurse cells. (D) At the mid-oogenesis, once *osk* mRNA reaches the posterior of the oocyte, Osk protein is expressed.

1.4.2.3 A higher order structure of *osk* mRNPs

As mentioned in the previous section, the BREs are crucial for *osk* mRNA translation repression. Interestingly, addition of exogenous Bruno proteins to an *osk* reporter construct containing BREs *in vitro* can provoke its oligomerization and formation of so-called silencing particles (50~80S) (Chekulaeva et al., 2006). In contrast, when the BREs in the reporter construct are mutated such that Bruno binding is strongly reduced or abolished, formation of the silencing particles fails, suggesting that, in addition to recruitment of Cup and repression at initiation via the cap-binding protein eIF-4E, Bruno protein can also repress through the BREs by assembling

silencing particles and repressing through a cap-independent mechanism (Chekulaeva et al., 2006). The *osk* mRNA translation repressors Me31B and Cup (see section 1.4.3) are both present in the silencing particles.

It has been suggested that the assembly of a higher order of *osk* mRNPs by the translation repressor Bruno is a new mechanism of mRNA translation repression that could be particularly suited for coupling translation repression with mRNA transport. Indeed, *osk* mRNA injected into cultured oocytes forms particles (Glotzer et al., 1997). Moreover, although it has been shown that 3'UTR is required for posterior localization of *osk* mRNA, it is not sufficient. Reporter construct bearing the *osk* 3'UTR only localize at the posterior pole in presence of the endogenous, spliced *osk* mRNA, suggesting that *osk* mRNAs are assembled via their 3'UTRs into transport complexes for localization (Hachet and Ephrussi, 2004; Kim-Ha et al., 1993). *Drosophila* PTB has been shown to be involved in the process of 3'UTR-dependent *osk* mRNA oligomerization (Besse et al., 2009). These lines of evidence suggest the existence of a higher order structure of *osk* mRNPs *in vivo*; however, the biological significance of particle assembly in the endogenous *osk* mRNA localization is still unknown.

1.5 Processing bodies

1.5.1 What are Processing bodies?

Similar to the notion that localization and translation repression of *osk* mRNA could happen in large complexes, a recently identified cytoplasmic granule in eukaryotes, called Processing body (P-body), has been suggested to be an aggregate of translationally inactive mRNPs and involved in mRNA degradation and translation repression.

The major pathway of mRNA decay is the 5' to 3' degradation (Parker and Song, 2004). The process of RNA degradation is initiated by deadenylation of the polyA tail and is predominantly mediated by the Ccr4/Pop2/Not complex. This is followed by a presumably irreversible process, called decapping, which removes the 5' cap structure of the mRNA. This is catalyzed by the decapping complex, containing Dcp1 and Dcp2, whose activity is stimulated by several

enhancers of decapping, including Dhh1/Rck/p54, Edc3, Lsm1 -7 complex and Ge-1. After losing its cap, the mRNA undergoes degradation from 5' to 3' by the exonuclease Xrn1. Interestingly, all of these proteins are enriched in P-bodies (Figure 7) (Eulalio et al., 2007a; Fillman and Lykke -Andersen, 2005; Ingelfinger et al., 2002; Parker and Sheth, 2007; Sheth and Parker, 2003) . In addition, P-bodies also contain components of the RNA-induced silencing complex (RISC), which is involved in microRNA -dependent repression (Liu et al., 2005) as well as translation repressors including 4E-T (Andrei et al., 2005; Ferraiuolo et al., 2005). Although the total protein composition of P -bodies has not been determined, the current list of P -body components reveals a close relationship between P -bodies and mRNA decay and repression.

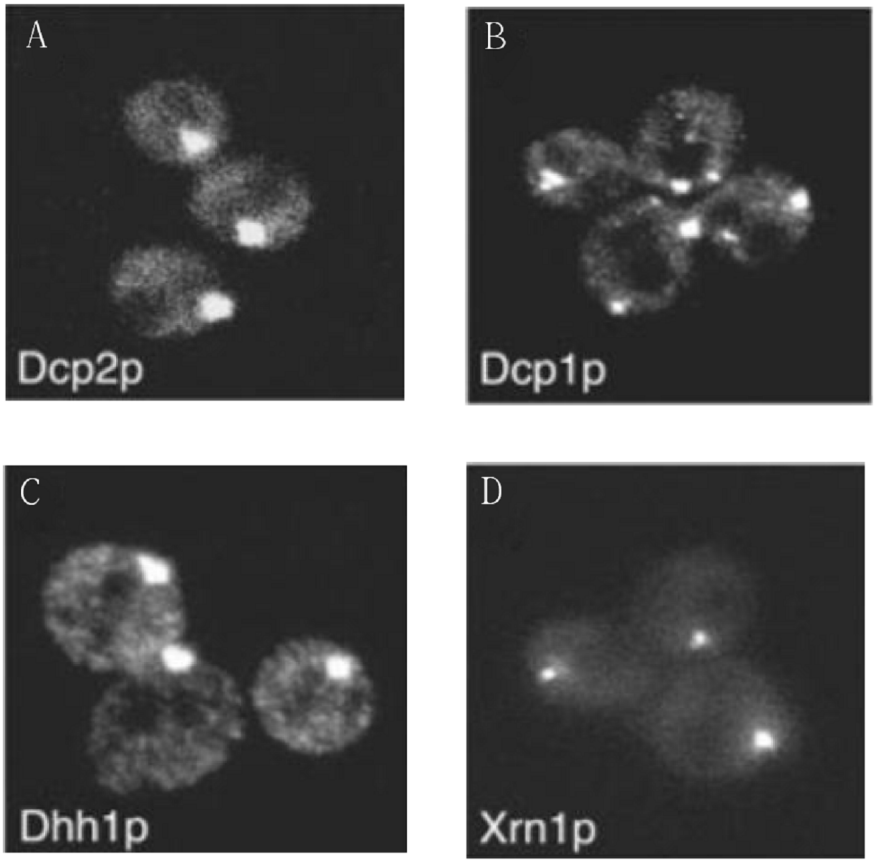

Figure 7 **Components of the 5' to 3' mRNA decay pathway localize to the P-bodies in yeast**

(A, B) In the yeast *S. cerevisiae* the decapping enzyme, Dcp2p, and its partner protein, Dcp1p, which together catalyze the removal of the 5' cap of mRNA, are enriched in P-bodies. (C) Dhh1p, an enhancer of decapping is also enriched in P-bodies. (D) Xrn1p, which hydrolyzes the decapped mRNA from 5' to 3', localizes to P-bodies. (Images from Sheth and Parker, 2003)

1.5.2 Biological function of P-bodies

Several lines of evidence suggest that P-bodies are the sites where mRNA decay and translation repression occur. Firstly, P-bodies contain mRNA decay intermediates and require RNA for their assembly. It has been observed that mRNAs into which an artificial strong secondary structure that impedes its degradation has been introduced are trapped in P-bodies (Sheth and Parker,

2003). Furthermore, RNAse A treatment of cells leads to the disruption of P-bodies *in vivo* (Teixeira et al., 2005). Secondly, P-bodies are dynamic structures whose number and size depend on the availability of mRNAs not associated with the translational machinery. For example, the entrapment of mRNAs in polysomes by inhibition of translation elongation with cycloheximide leads to the disappearance of P-bodies (Cougot et al., 2004; Liu et al., 2005; Sheth and Parker, 2003; Teixeira et al., 2005). Conversely, the release of mRNAs from polysomes by inhibition of translation initiation through the addition of puromycin, which increases the proportion of untranslated mRNAs in the cell, provokes P-body formation (Eulalio et al., 2007b). Consistent with this, when a cell is placed under conditions of stress, such as nutrition depletion, which causes a general repression of translation, the formation P-bodies is promoted (Brengues et al., 2005). Finally, when the flux of mRNA degradation is perturbed, P-bodies change in number and size. For example, the obstruction of mRNA decay at an early step, such as deadenylation, which reduces the amount of mRNA entering the degradation pathway, causes a reduction in P-body number (Eulalio et al., 2007b; Sheth and Parker, 2003). In contrast, blocking the final 5' to 3' degradation, which leads to accumulation of decapped mRNAs, promotes P-body formation (Cougot et al., 2004; Sheth and Parker, 2003).

P-bodies have been identified in many species, including yeast, humans, flies and plants (Cougot et al., 2004; Eulalio et al., 2007b; Gallo et al., 2008; Xu et al., 2006). Considering that mRNA decay and translation repression happen in P-bodies, it was thought that the formation of P-bodies might play a crucial role in these processes. However, several recent studies have shown that the knockdown of microscopy-detectable P-bodies has no obvious effect on either mRNA decay or translational repression (Decker et al., 2007; Eulalio et al., 2007b). Thus, the biological role of P-bodies as structures remains unclear. Taking this into account, it has been proposed that the function of P-bodies might be to compartmentalize the mRNA decay and translation repression machineries into small areas, thereby enhancing the robustness of these processes.

Finally, most of the studies regarding P-body function were addressed in cells in culture or the single cell eukaryote, *S. cerevisiae*. Hence the function of P-bodies in a multicellular organism has remained largely unknown .

1.5.3 mRNA cycle between P-bodies and the polysomes

Strikingly, mRNAs that are translationally repressed in P-bodies can also exit these structures and reenter the translated mRNA pool (Bhattacharyya et al., 2006; Brengues et al., 2005). For example, when yeast cells transit from the stationary phase to the growth state, P-bodies are reduced in number and size, and the mRNAs contained within them shift to the polysomes. Considered with the fact that the number and size of P-bodies depend on the availability of untranslated mRNAs, this suggests an intriguing dynamic model of the movement of mRNAs between the polysomes and P-bodies, depending on their translation status (Figure 8). When the balance of mRNA status favors translation inactivation, mRNAs become dissociated from the polysomes and associate with mRNA translation repression or degradation machineries to form complexes that further assemble into P-bodies. Conversely, when translation is favored, mRNAs exit the P-bodies to associate with ribosomes, and both the size and number of P-bodies decline.

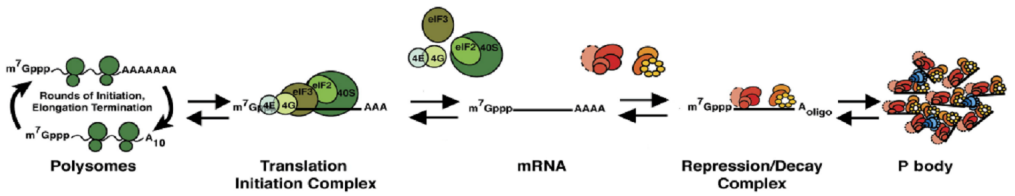

Figure 8 **A dynamic movement of mRNA between P-bodies and translational machineries**

Depending on its translation state, an mRNA can move between P-bodies and translational machineries by either associating with the translation initiation complex for its translation or interacting with repression factors and P-body components to be assembled into P-bodies. (Adapted from Parker and Sheth, 2007)

1.5.4 Molecular mechanism of P-body assembly

The formation of P-bodies has been proposed to be a self-assembly event (Franks and Lykke-Andersen, 2008; Parker and Sheth, 2007). In yeast, two P-body components, Edc3, containing an Yjef-N dimerization domain, and

Lsm4, containing a prion-like Glutamine/Asparagine (Q/N)-rich domain, were shown to be required for P-body assembly by promoting the physical interaction between mRNPs (Decker et al., 2007; Reijns et al., 2008). The simultaneous deletion of both domains in the respective proteins causes the complete loss of P-body formation, suggesting that self-aggregation domains play an important role in P-body assembly. The Yjef-N domain of Edc3 is highly conserved among different eukaryotic species, suggesting that Edc3 has a similar function in other eukaryotes. However, the Q/N domain of yeast Lsm4 is not found in its other eukaryotic homologues, suggesting that Lsm4 either performs its function by a different mechanism or does not promote P-body formation in these organisms. Interestingly, a conserved protein Ge-1 with no homologue in yeast contains such a Q/N domain at its C-terminus (Decker et al., 2007), and has been shown to be required for P-body formation in human and *Drosophila* cells (Eulalio et al., 2007b; Yu et al., 2005). In addition, overexpression of the *wild-type* Ge-1 protein can induce the formation of the aberrant P-body-like structures in mammalian cells (Fenger-Gron et al., 2005). Taken together, these suggest that Ge-1 plays a crucial role in P-body formation in higher eukaryotes.

1.6 Ge-1 protein

Ge-1 was first identified as a target of an auto-antiserum from a patient with Sjögren's syndrome, in which immune cells attack and destroy the exocrine glands that produce tears and saliva (Bloch et al., 1994). Later, it was shown that Ge-1 is also an antigen in another autoimmune disease, Primary biliary cirrhosis, which is marked by the slow progressive destruction of the small bile ducts within the liver (Yu et al., 2005). However, a clear relationship between Ge-1 and the clinical syndrome of these autoimmune diseases has not yet been established.

Proteins of the Ge-1 family contain an N-terminal WD40 repeat domain (Fenger-Gron et al., 2005; Xu et al., 2006; Yu et al., 2005), which is often involved in protein-protein interaction (Li and Roberts, 2001), a serine-rich low-complexity linker and a C-terminal prion-like Q/N-rich domain (Figure 9 and see section 1.5.2) (Decker et al., 2007). In *Homo sapiens*, *D. melanogaster* and *Arabidopsis thaliana*, Ge-1 protein localizes to P-bodies and

is required for P-body integrity (Eulalio et al., 2007c; Fenger-Gron et al., 2005; Xu et al., 2006; Yu et al., 2005). Deletion analysis of Ge-1 protein in fly, plant and mammalian cells has revealed that its C-terminal domain is necessary and sufficient for its P-body localization (Eulalio et al., 2007c; Xu et al., 2006; Yu et al., 2005). Moreover, the *Arabidopsis* Ge-1 can form dimers/multimers through the C-terminal domain, which fits with the putative prion-like property of the Q/N-rich motif within it (Xu et al., 2006). Hence, together with its high molecular weight (around 150 kDa), Ge-1 has been speculated to function as a scaffold protein that recruits other factors.

In humans and *Arabidopsis*, Ge-1 associates with Dcp1 and Dcp2 and enhances their decapping activity, although the molecular mechanism of Ge-1 action is still unknown (see section 1.5.1) (Fenger-Gron et al., 2005; Xu et al., 2006). In addition, the co-depletion of *Drosophila* Ge-1 together with other proteins involved in decapping, such as Me31B and Dcp1 can partially release miRNA-based repression of some transcripts, suggesting that Ge-1 might be involved in the miRNA-silencing pathway (Eulalio et al., 2007c). Moreover, it has been suggested that *Arabidopsis* Ge-1 is involved in postembryonic development through the regulation of the decapping process (Xu et al., 2006). However, the *in vivo* function of Ge-1 in metazoans remains elusive.

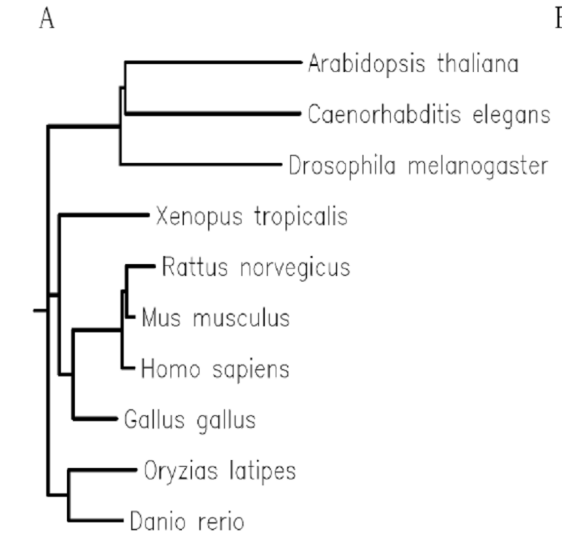

B

	N-terminal	C-terminal
H. sapiens	31%(51%)	28% (51%)
M. musculus	31%(52%)	27% (51%)
D. rerio	29%(50%)	27% (52%)
C. elegans	24%(42%)	26% (49%)
A. thaliana	21%(38%)	23% (42%)

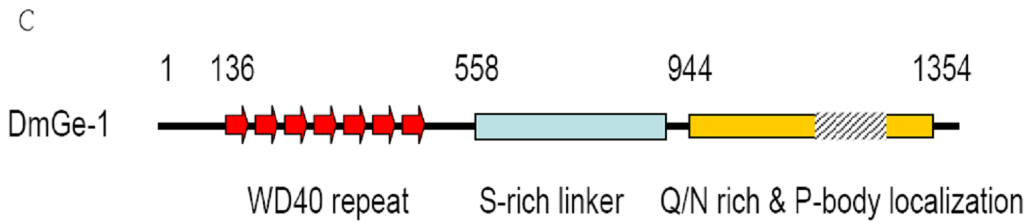

Figure 9 **Ge-1, a conserved protein in multicellular eukaryotes**

(A) Phylogenetic tree of the Ge-1 protein family. Determination of the evolutionary relationships among Ge-1 homologues was based on the multiple sequence alignment of different Ge-1 proteins using CLUSTALW. (B) The degree of identity and similarity (shown in parenthesis) of the N-terminal and C-terminal regions of *Drosophila* Ge-1 and its homologues. (C) A diagram of the architecture of *Drosophila* Ge-1 protein. The N-terminal region contains seven predicted WD40 motifs (red arrows). The central part (gray) is serine-rich and shows low complexity. The C-terminal region (yellow) contains a Q/N-rich motif (from amino acid 1106 to 1230, black shadow) and is required for Ge-1 localization to P-bodies. Numbers above the protein indicate the amino acid positions at the fragment boundaries.

1.7 Aim of the thesis

Initially shown to be involved in *osk* mRNA regulation and components of *osk* mRNPs, dDcp1, Me31B, and Cup were later found in P-bodies, indicating a close relationship between the *osk* transport granules and P-bodies. In addition, just as for P-bodies, recent evidence suggested that, during transport, *osk* mRNAs can assemble into translationally repressed mRNA granules. One speculation therefore was that P-bodies and *osk* transport granules might be similar RNA granules, derived from a prototype granule consisting of basic components that execute similar functions in both types of granule. The RNA granules would then be adapted to their specific functions, by recruitment of different accessory proteins. Hence, it was of interest to know if other important P-body components are involved in *osk* mRNA regulation. To address this question, in view of the fact that Ge-1 plays a crucial role in P-body assembly in both mammalian and *Drosophila* cells, I decided to focus on *Drosophila Ge-1* (*dGe-1*) and to explore its function *in vivo,* during oogenesis. The aims of my thesis were, first, to generate a *dGe-1* mutant – as there was no mutant available, second, to test the *in vivo* function of *dGe-1* in P-body formation, and third, to investigate the possible involvement of *dGe-1* in *osk* mRNA regulation.

2. Materials and methods

2.1 Fly genetics

2.1.1 Fly husbandry

Flies *(D. melanogaster)* were grown on standard corn meal molasses agar (1L water mixes with 12g agar, 18g dry yeast, 10 soy flour, 22g turnip syrup, 80g corn powder, 6.25ml propionic acid, and 2.4g methyl 4-hydroxybenzoate). All crosses were performed at 25 □. Fly stocks were kept at 18 □ and flipped once per month.

2.1.2 Fly stocks

In this study I made use of the following fly stocks: w^{1118}, used as a *wild-type* control, *YFP-dDcp1* (Lin et al., 2006), *EGFP:Me31B* (Nakamura et al., 2001), *maternal-α-tubulin-Gal4:VP16* (Hacker and Perrimon, 1998), *w; P[SUPor-P] KG05826* (Bloomington stock collection ID: 14124), *w; P[w[+mC]=GSV2] GS5005* (Kyoto stock collection ID: 200633)

2.1.3 Generation of transgenic flies

Transgenic flies were generated by P element-based transformation (Rubin and Spradling, 1982) using the pCasper4 (from the Drosophila Genomic Resource Center: ID 1213) or pUASp vector (Rorth, 1998). Integration of the injected transgenic constructs in the genome of recipient flies is randomly induced by P element transposase expressed from the co-injected plasmids.

2.1.4 Generation of *dGe-1* deletion alleles by imprecise excision

The P elements bearing the mini-white gene in two fly stocks, KG05862 and GS5005, were remobilized by crossing with the w/w; If/CyO; Δ2-3, Sb /TM6B flies, in which the P element transposase is constitutively expressed. In the germline as well as the soma of the F1 progenies bearing both the P element and the transposase, both imprecise and precise excision could happen. Each F1 male then mated with 3~4 w/w; If/CyO females in separated vials to

disseminate the male gametes. From each vial, single deletion candidate male, recognized by the white-eye-color, was selected for crossing with the original P element / CyO females. A single fly PCR screen (see section 2.2.1) with three sets of primers, Ge-1 806F/ Ge-1 1302R, Ge-1 806F/ Ge-1 1676R, and Ge-1 806F/ Ge-1 2626R (for their sequences see section 2.2.6) against the genomic region of *dGe-1*, was subsequently performed on the F3 progeny to identify the possible deletion alleles of *dGe-1*. Another two pairs of primers were used to check for the existence of the P element (for KG05862, two pairs of primers were P5'/ Ge-1 806F and P3'/ Ge-1 2626R. For GS5005, they were P5'/ Ge-1 2626R and P3'/ Ge-1 806F. For their sequences see section 2.2.6). Finally, the deletion region of the *dGe-1* mutations was further mapped by sequencing and the lethality was examined genetically. For the cross scheme, see Figure 10.

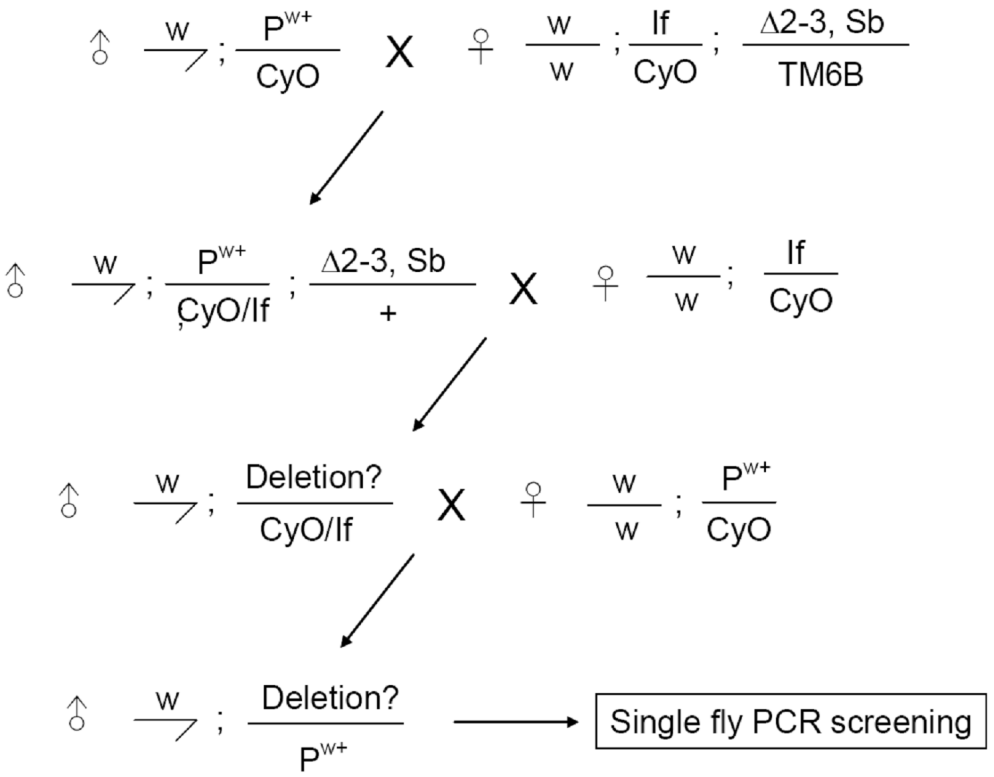

Figure 10 The crossing scheme for P element imprecise excision

2.1.5 Generation of germline clones by the FLP-DFS technique

A given gene can have different biological functions at different stages of development, and the early death of a mutant organism due to a lethal mutation can hamper the analysis of the gene function during later development. To circumvent this difficulty, in fly the FLP/FRT technique was developed to enable generation of homozygous mutant cell clones in an otherwise heterozygous fly (Golic, 1991). Flippase (FLP), a recombinase identified in *S. cerevisiae*, can induce the recombination between two Flippase Recognition Target (FRT) sites. To generate the mutant cell clones, a mutant allele of a gene of interest is recombined onto homologous FRT-containing chromosome. Recombinant flies in which the mutant allele is now on an FRT-bearing chromosome are then crossed with flies bearing a heat -inducible FLP and a dominant maker (e.g. GFP) on the homolgous FRT chromosome . During development, the F1 progeny are challenged by two heat shocks for one-hour each at 37□ on two successive days, to induce the mitotic recombination between the homologous chromosomes at the FRT sites. The recombination gives rise to a homozygous mutant cell lacking the dominant marker, as well as a *wild-type* cell bearing two copies of the dominant marker. After cell division, these two cells will poliferate and generate two distinct clusters (clones) of cells within the other, mainly heterozygous cells . For the generation of the mutant clones in the germline, a similar technique, called FLP-DFS (Dominant Female Sterile), is used (Figure 11) (Chou and Perrimon, 1996). Ovo^{D1}, whose expression in the germline leads to an early arrest of oogenesis, is used as the dominant marker. As a result, only the homozygous mutant germline cells that do not express Ovo^{D1} can complete the oogenesis, allowing the easy sellection of the mutant egg-chambers.

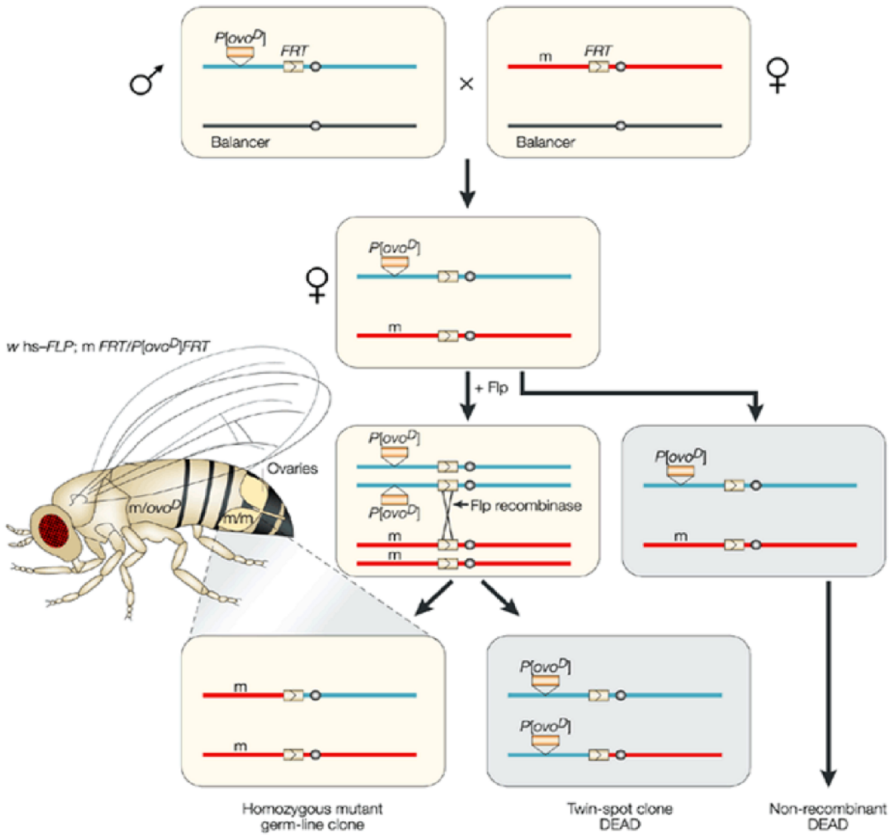

Figure 11 **The FLP-DFS technique**

A fly bearing one pair of homologous chromosomes, one of which (the blue chromosome) bears a suitable Flippase Recognition Target (FRT) site and a mutation in the gene of interest, and the other (the red chromosome) also contains a suitable FRT and the ovo^{D1} Dominant female sterile (DFS) mutation, is generated by genetic cross. During its development, the flip recombinase (or Flippase, Flp) driven by heat-shock induces mitotic recombination between the paired FRT sites. In the germline, this recombination event results in the generation of a homozygous mutant clone, as well as a "twin-spot" *wild-type* clone, among the otherwise heterozygous cells. Because only the homozygous mutant clone has no ovo^{D1}, which kills germ cells during early oogenesis, the germ cells of all the surviving egg chambers are homozygous. hs, heat shock; m, mutation; *w*, *white* gene. (Image from St Johnston, 2002)

2.1.4 Ectopic expression using the Gal4-UAS system

The Gal4-UAS system is a powerful genetic tool to express a gene of interest in a specific pattern in the fly (Brand and Perrimon, 1993). Identified in the yeast *S. cerevisiae*, Gal4 encodes a transcription factor that specifically binds to a 17 base-pair Upstream Activating Sequences (UAS) to activate the expression of the downstream gene (Giniger et al., 1985). Then this bipartite system was adapted for use in *Drosophila*, and requires two types of flies, one expressing GAL4 under the control of a promoter selected for its pattern of activity (e.g. stage or tissue specific) and the other bearing 14 repeated UAS sequences immediately upstream of a gene of interest. By crossing the two kinds of flies, one can select progeny bearing both the GAL4 transcription activator and UAS-target gene moieties, and thus express the gene of interest in the desired spatial and temporal pattern. For the ectopic expression in the germ-line, a modified UASp was developed (Rorth, 1998).

2.2 Molecular biology

2.2.1 Single fly PCR

A single fly was squashed in 50 µl SB buffer (10 mM Tris-Cl, 1 mM EDTA, 25 mM NaCl, 200 µg/ml Proteinase K). The sample was first incubated for 20-30 minutes at 37°C, then at 95°C for 2 minutes to inactivate the proteinase K. The sample then was stored at 4°C for weeks.

1 µl of sample was used in a final volume of 10 µl standard PCR reaction solution. The PCR reaction was carried on a Thermal Cycler (PTC-200, MJ research) according to the following program: (1) 94°C for 10 minutes, (2) 94°C for 1 minute, (3) 55°C for 1 minute, (4) 72°C 30 seconds/ kb (depends on the length of the product), (5) repeat step (2)-(4) for 30 times, (6) 72°C 10 min, (7) end.

The amplified products then were analyzed by agarose gel electrophoresis and visualized with SYBR SAFE staining (Invitrogen).

2.2.2 RNA isolation

10 pairs of ovaries from adult flies were dissected in cold PBS and then disassociated in 200 µl of Trizol (Invitrogen). An additional 600 µl of Trizol was added and the RNA was isolated according to the manufacturer's instructions.

2.2.3 cDNA synthesis and RT-PCR

cDNA was synthesized using the ThermoScript RT-PCR System (Invitrogen), following the manufacturer's instructions with 1~3 µg RNA and oligo(dT) primers incubated at 55°C for 45 min. The cDNA product was used in a 10 µl standard PCR reaction. To detect the presence of *dGe-1-A* and *dGe-1-B* transcripts in the ovary, the primer set, Ge-1 1166F/ Ge-1 1420R (for their sequences see section 2.2.6) was used. For the examination of the level *dGe-1* transcript expression three sets of primers (Ge-1coding 502F/ Ge-1coding 899R, Ge-1coding 2037F/ Ge-1coding 2352R and Ge-1coding 3070F/ Ge-1coding 3345R; for their sequences see section 2.2.6) complementary to different regions of *dGe-1* transcript were used. As a control, *rp49* was amplified using the primer set, Rp 49 F/ Rp 49 R (for their sequences see section 2.2.6). The amount of amplified products was then analyzed by standard agarose gel electrophoresis, followed by SYBR-SAFE staining (Invitrogen).

2.2.4 Cloning of UASp-Flag:HA:dGe-1

The dGe-1 coding region was amplified by PCR, using the primer set, Ge-1 gateway F and Ge-1 gateway R (for the sequences see section 2.2.6), and EST clone LD32717 as a template. The amplified fragment was cloned into pENTR/D-TOPO, using the Gateway System (Invitrogen) and successful cloning verified by sequencing. The dGe-1 coding region was cloned by recombination (Gateway Technology, Invitrogen) from the pENTRY construct into the UASp-based destination vector pPFHW (The Drosophila Gateway Vector Collection). Cloning into pPFHW results in addition of 3 Flag tags and 3 HA tags at the N-terminus of the insert. The final construct was used to generate transgenic stocks by germline-mediated transformation (see section 2.1.3).

2.2.5 Cloning of the dGe-1 cDNA rescued construct

A full-length cDNA of *dGe-1* was generated by PCR using the primer set, Ge-1 cDNA F/ Ge-1 cDNA R (for their sequences see section 2.2.6). Ge-1 cDNA F primer and R primer contain one Not I and one XbaI restriction sites, respectively, added for future cloning purposes. The amplified fragment was digested with Not I and XbaI, and then ligated to a Not I and XbaI digested pCaseper4-tubulin vector (gift of Stephen Cohen's lab) which was also digested with Not I and XbaI. The resulting construct was validated by sequencing and then used for generation of transgenic stocks by germline-mediated transformation (see section 2.1.3).

2.2.6 Primer list

Name	Sequence
Ge-1 806F	**CCACCACACACAATCACAC**
Ge-1 1302R	**CCTATCAATACGCAGCAGTC**
Ge-1 1676R	**ACGCACATGACTTCTATTTCC**
Ge-1 2626R	**ATTAGCACAAACGAACCCC**
P3’	**ACTCAATACGACACTCAGAATACT**
P5’	**CACCCAAGGCTCTGCTCCCACA AT**
Ge-1 1166F	**TTTACGAGAAGCAGCCAAC**
Ge-1 1420R	**AGAGCGCGATTAACATTGAC**
Ge-1 cDNA F	**GAGCGGCCGC ACACGCCGCTACACACCTCTA**
Ge-1 cDNA R	**GGTCTAGAAAAATAATAAAAAAATATATTGCA**
Ge-1 gateway F	**CACCATGTTAATCGCGCTCTTCGCGC**
Ge-1 gateway R	**TTTTAGCTGATCGCGGTACGTTAT**
Ge-1coding 502F	**GCATGGTGCGCGTATGCAAC**
Ge-1coding 899R	**GCTGCTGGTTGGATCTTGCC**
Ge-1coding 2037F	**ACCACCAGCGGTCAGGATAG**
Ge-1coding 2352R	**CTCTGCTTCGTAGGCATCGG**
Ge-1coding 3070F	**TCAACATGGAACTGCAGCGCC**
Ge-1coding 3345R	**TATGCCCACGCTGAAAGCGTC**
Rp 49 F	**GCTAAGCTGTCGCACAAA**
Rp 49R	**TCCGGTGGGCAGCATGTG**

2.3 Generation of Rabbit α-dGe-1 antibody

The dGe-1 C-terminal region (a.a. 1220-1354) was expressed from pETM60:dGe-1 plasmid by the EMBL Protein Expression and Purification core facility as previously described (Jinek et al., 2008). The resulting peptide, mixed with TiterMax Gold adjuvant (Sigma), was injected into rabbits by the EMBL Laboratory Animal Resources (LAR), who also performed the

subsequent boosts and bleeds. The bleeds were clotted at room temperature for 30 min and centrifuged at 2500g. The supernatants were collected as the anti-dGe-1 antiserum and kept at 4°C, with addition of 0.02% sodium azide for short-term storage and at -80°C for long-term storage.

2.4 Western Blotting

Ovarian extracts were obtained by manually dissociating five pairs of ovaries in 2x SDS–polyacrylamide gel electrophoresis (SDS–PAGE) sample buffer. For embryonic extracts, embryos were first dechorinated in 50% sodium hypochloride for 1-3 minutes, then washed twice in PBS and finally homogenized in 2x SDS–PAGE sample buffer. Samples were then boiled at 95°C for 5 minutes and stored at -20°C for further use.

Proteins were separated on 8% SDS-polyacrylamide gels by electrophoresis with a constant current of 15 mA per mini-gel, and then transferred to PVDF membrane Imobilon-P (Millipore, cat. no. IPVH00010) using a constant voltage of 100V for 1 hour or a constant current at 120 mA over night. The membrane was blocked with 5% BSA in TBS (50mM Tris pH 7.5, 150 mM NaCl, 0.2% Tween-20) for 1 hour. Next, the membrane was incubated with primary antibody diluted in 5% BSA/TBS at 4°C over night. The following primary antibodies were used: rat anti-dGe-1 (1:1000, 1:1000 gift of Elisa Izaurralde), rat anti-Cup (1:500, gift of Akira Nakamura), rabbit anti-Kinesin heavy chain (1:50000, Cytoskeleton), rabbit anti-GFP (1:50000, Torrey Pines Biolab), rabbit anti-Exu (1:20000, gift of Paul Macdonald), mouse anti-Me31B (1:1000, gift of Akira Nakamura), mouse anti-Tubulin (1:10000, DM1A, Sigma), mouse anti-HA (1:1000, HA.11, Convance). The membrane was rinsed once, and washed three times for 15 minutes in TBS. The membrane was next incubated with the HRP-conjugated secondary antibodies (GE Healthcare), diluted in 5% BSA /TBS for 1 hour at room temperature. The membrane was washed three times for 15 minutes in TBS and then rinsed with the enhanced chemiluminescence reagent by mixing equal volumes of the Enhanced Luminol Reagent and the Oxidizing Reagent (NEL105, PerkinElmer). The membrane was exposed to Kodak X-OMAT MR Film for 10 seconds to 5 minutes.

2.5 Co-immunoprecipitation

Ovaries from 70 female flies were homogenized in 100 µl DXB-150 buffer (25 mM Hepes-KOH pH 6.95, 250 mM sucrose, 1 mM $MgCl_2$, 1 mM DTT, 150 mM KCl, 0.1% Triton X-100) containing complete Protease inhibitor cocktail EDTA free (Roche), and centrifuged at 10000g for 10 minutes at 4□. For the GFP-tagged protein pull-down, the supernatant was first incubated with 5 µl rabbit anti-GFP antibody (Torrey Pines Biolab) at 4□ over night on a head-over-tail rotor and then with 30 µl protein A sepharose beads (Amersham) at 4□ for 2 hours.

After immunoprecipitation, the beads were washed 6 times for 10 min with 500 µl DXB-150, the proteins were then eluted in 2X SDS–PAGE sample buffer 10 min at 95□, and analyzed by western blotting (see section 2.4).

For the RNAse A sensitivity assay, RNAse A was added into ovarian extracts at a concentration of 0.33 µg/µl.

2.6 Immunohistostaining

2.6.1 Immuno-fluorescent staining of *Drosophila* egg-chambers

Ovaries were dissected from females in cold PBS and fixed in 4% formaldehyde in PBST (PBS with 0.1% Tween-20) for 20 minutes. After washing with PBST twice for 10 minutes, ovaries were permeabilized in PBS with 1% Triton-X for 1 hour, and then blocked in the blocking buffer (PBST with 0.5% BSA) for 3~4 hours. Ovaries were incubated overnight with primary antibody in the blocking buffer. Primary antibodies used in this study: rat anti-Staufen (1:2000), rabbit anti-Me31B (1:4000, gift of Akira Nakamura), rabbit anti-trailer hitch (1:1500, gift of Akira Nakamura), mouse monoclonal anti-Cup (1:1000, gift of Akira Nakamura), rat anti-dGe-1 (1:1000, gift of Elisa Izaurralde), mouse monoclonal anti-HA (1:500, HA11, Convance).

Ovaries were washed twice for 20 minutes in PBST, and then blocked in PBST with 10% normal goat serum (NGS) for 1 hour before incubation with Cy3

(1:500) or Cy5 (1:500) conjugated secondary antibodies in PBST with 10% NGS for 2 hours. Ovaries were washed repeatedly in PBST, and mounted in mounting medium (2% n-propylgallate, 80% glycerol). Images were taken using a Leica SP2 confocal microscope and edited using Adobe Photoshop CS.

2.6.2 Simultaneous visualization of protein and RNA by *in situ* hybridization coupled with immunodetectio

Immunostaining of proteins coupled with RNA *in situ* hybridization was carried out as previously described (Vanzo and Ephrussi, 2002). Rabbit anti-Osk (1:3000) and Digoxigenin-labeled *osk* antisense probe (1:30000) were used.

2.7 Determination of unhatching rates

Flies were allowed to lay eggs for up to 12 hours. After removal of the flies, the eggs then were incubated at 25°C for 36 hours. The hatching rate was assayed essentially as previously described (Coutelis and Ephrussi, 2007).

2.8 Cuticle preparation

The unhatched eggs were dechorionated in a 50% sodium hypochloride solution for 2 minutes, then washed twice in H_2O, mounted in Hoyer's medium, and finally baked overnight at 65°C (Wieschaus et al., 1984).

2.9 *in situ* electron microscopy

in situ electron microscopy was carried out by Alvar Trucco essentially as previously described (Delanoue et al., 2007). Rat anti-dGe-1 (1:10) Dig-labeled and *osk* anti-sense probe were used.

2.10 Websites

- Ensembl http://www.ensembl.org/
- FlyBase http://flybase.bio.indiana.edu/
- BLAST http://www.ncbi.nlm.nih.gov/BLAST/
- ClustalW http://www.ebi.ac.uk/clustalw/index.htm
- Drosophila Gateway collection
  http://www.ciwemb.edu/labs/murphy/Gateway%20vectors.html
- SDSC biological workbench http://workbench.sdsc.edu/

3. Results

3.1 *dGe-1* is expressed during oogenesis

The *dGe-1* locus spans approximately 5.5 kb in *Drosophila*. Sequencing of full-length cDNA clones of *dGe-1* from the embryo revealed that the *dGe-1* locus encodes two transcripts, *dGe-1-A* and *dGe-1-B* of 4624 nt and 4707 nt, respectively (Figure 12A). The two transcripts only differ in their 5'UTR. In the *dGe-1-B* transcript, the first intron of *dGe-1-A* is not spliced, resulting in a longer 5'UTR. To test whether both *dGe-1* transcripts are expressed during oogenesis, I performed RT-PCR using a pair of primers which flank the alternatively spliced intron to assess the presence of each *dGe-1* transcript in *wild-type* ovarian extract (Figure 12A, the brown primers). The result showed that both of the transcripts could be detected, suggesting that they are transcribed during oogenesis (Figure 12B).

These two *dGe-1* transcripts are translated into a single protein of approximately 150 kDa (1354 aa.), as was shown by western blotting using a rat anti-dGe-1 antibody that recognizes the C-terminal domain of dGe-1 in *Drosophila* S2 cell extract (Eulalio et al., 2007c). To determine if dGe-1 protein is present in the germline, I performed western blotting using the same antibody on an extract of 0~2 hr embryos, whose content is essentially that of the oocyte, as the somatic follicle cells have degenerated during late oogenesis and the transcription of the zygotic genome has not yet begun. However, two major bands around 150 kDa were observed in this extract (Figure 12C). One possible explanation is that one of them does not correspond to dGe-1, as only a single isoform of Ge-1 protein is detected in *Drosophila* S2 cells as well as in the many other mammalian cell lines (Eulalio et al., 2007b; Yu et al., 2005). Other possibilities are that both bands represent dGe-1 protein, which could be subject to posttranslational modification or that two dGe-1 proteins are produced by the usage of different translation initiation codons. In order to study the function *dGe-1* during oogenesis and to test if both bands correspond to dGe-1 protein, a *dGe-1* mutant in which the level of dGe-1 protein is reduced was needed.

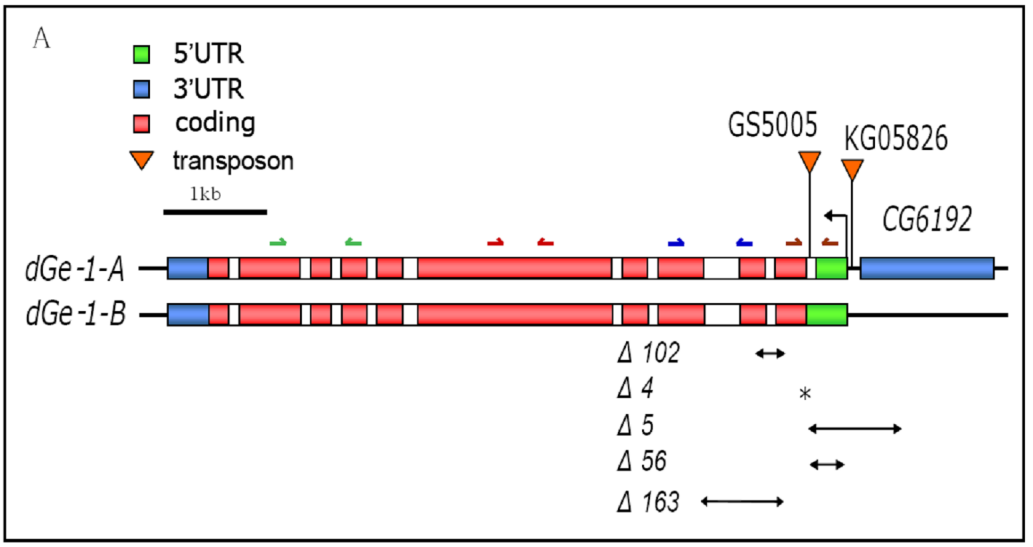
A
5'UTR
3'UTR
coding
transposon
1kb
GS5005
KG05826
CG6192
dGe-1-A
dGe-1-B
Δ 102
Δ 4
Δ 5
Δ 56
Δ 163
*

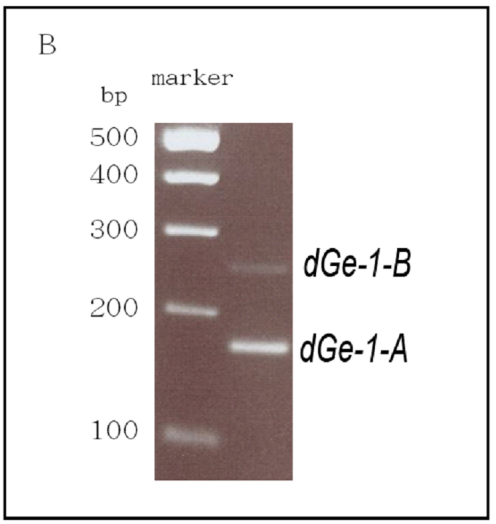
B
marker
bp
500
400
300
200
100
dGe-1-B
dGe-1-A

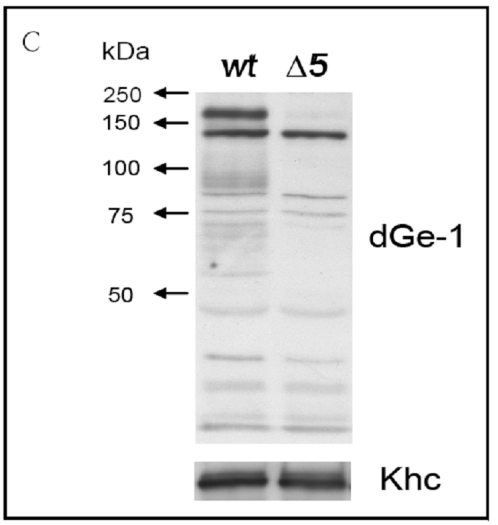
C
kDa
wt
Δ5
250
150
100
75
50
dGe-1
Khc

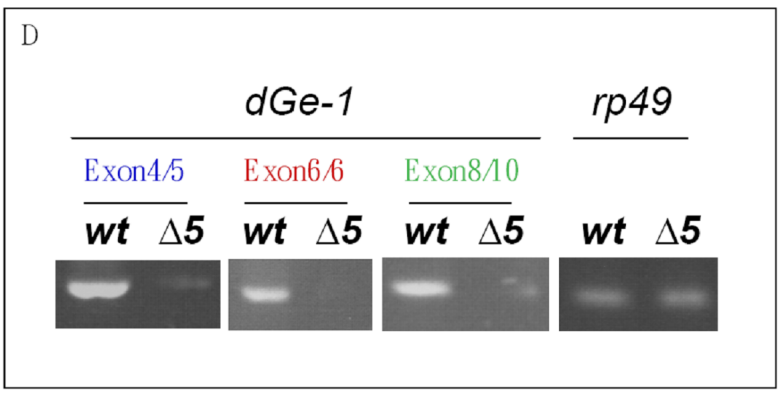
D
dGe-1
rp49
Exon4/5
Exon6/6
Exon8/10
wt
Δ5
wt
Δ5
wt
Δ5
wt
Δ5

Figure 12 ***dGe-1* is expressed during oogenesis**

(A) Schematic representation of the *dGe-1* locus at polytene band 32D3. The insertion sites of two P-element transposons used for the generation of *dGe-1* deletion alleles, as well as the deleted regions in the deletion alleles (double-head arrows) are represented. The small, colored half-arrows represent the positions of the primers used for RT-PCR. (B) During oogenesis, two *dGe-1* transcripts were detected by RT-PCR. A set of primers flanking the alternatively spliced intron (the brown primers in A) was used to detect the two transcripts of *dGe-1* simultaneously. In the ovarian total RNA extract, two PCR products of a length of 171 bp and 254 bp, which represent the *dGe-1-A* and *-B*, respectively, were observed. (C) Western blot analysis using anti-dGe-1 antibody showing that a band just above 150 kDa is specifically absent in the $dGe\text{-}1^{\triangle 5}$ mutant, compared with *wild-type* early embryonic extract. A non-specific band just below 150 kDa was observed in both genotypes. Khc: loading control. (D) *dGe-1* transcript was dramatically reduced in the $dGe\text{-}1^{\triangle 5}$ *GLC* ovaries. Three sets of primers (the blue, red, and green primers in A) were used in RT-PCR to detect the *dGe-1* transcript in *wild-type* and $dGe\text{-}1^{\triangle 5}$ *GLC* ovaries. *rp49* served as a loading control.

3.2 Generation of *dGe-1* mutant alleles

3.2.1 Imprecise P element excision generates five *dGe-1* alleles

P element remobilization by transposition has been widely used to produce small deletions around the P element transposon insertion site. I therefore sought and obtained two fly stocks, KG05826 and GS5005, bearing a P element near to and within the *dGe-1* locus, respectively, from the *Drosophila* stock centers. Strain KG05826 contains a P element inserted 39 bp upstream of the transcription start site of *dGe-1*, while in GS5005 the P element is inserted at 34 bp upstream of the translation start site of *dGe-1*, within the first intron of *dGe-1-A*. Both P element constructs contain a *mini-white* marker gene, such that presence of the P element can be recognized by the red eye-color produced in the w^- flies. The genetic scheme used to remobilize the P elements is shown in Figure 10. Remobilization of the P elements was induced by introducing Δ2-3 P element transposase into the P element-containing flies through a genetic cross. Around 680 males both bearing the P element chromosome and expressing the transposase were generated, then mated with female flies to disseminate their gametes for screening. In the following

generation, any white-eyed progeny - possibly reflecting imprecise excision of the P element - was selected for deletion analysis. Three sets of primers flanking the P element insertion sites, covering ~500 bp, ~800 bp and ~1.6 kb of the *dGe-1* locus, were used to examine the sequences flanking the P element insertion site for alterations caused by P element excision . In addition, two other sets of primers were used to further check the absence of the P elements in these selected flies. As a result, five *dGe-1* deletion alleles (*dGe-1* ^{102}, *dGe-1* ^{163}, *dGe-1* ^{4}, *dGe-1* ^{5} and *dGe-1* ^{56}) were identified from this screen and the extent of the deletions was mapped by sequencing (Table1, Figure 12A).

Table 1 **List of *dGe-1*deletion alleles generated in this study, by imprecise excision of P element**

The number in the deletion position column indicates the relative position to the transcription start site of the *dGe-1* locus.

Name	Deletion position	Corresponding region in the *dGe-1* locus	Lethality
Δ*102*	+540 ~ +728	Coding	Semi-lethal
Δ*4*	+302 ~ +306	Splicing acceptor site	Lethal
Δ*5*	-448 ~ +273	5'UTR, intergenic region, 3'UTR of CG6192	Lethal
Δ*56*	+71 ~ +273	5'UTR	Viable
Δ*163*	+302 ~ +946	Coding	Lethal

3.2.2 *dGe-1* ^{5} is a strong hypomorphic *dGe-1* deletion allele

Genetic testing revealed that *dGe-1* ^{56} was viable and *dGe-1* ^{102} was semi-lethal, whereas *dGe-1* ^{4}, *dGe-1* ^{5} and *dGe-1* ^{163} mutants were recessive lethal (Table 1), indicating that these three mutations were genetically strong *dGe-1* alleles and *dGe-1* is an essential gene in *Drosophila*.

To determine the relative allelic strength of these three *dGe-1* alleles, I examined the lethal phase of the homozygous larvae. While some of the *dGe-1* ^{163} homozygotes could survive until eclosion but remained trapped in the pupa cases, few *dGe-1* ^{4} and *dGe-1* ^{5} homozygous larva survived to the eclosion stage. This suggests that *dGe-1* ^{4} and *dGe-1* ^{5} are stronger alleles than *dGe-1* ^{163}. In order to determine how much of the *dGe-1* gene was deleted by the P element excision, I sequenced the genomic region flanking the original P element insertion sites in the *dGe-1* ^{4} and *dGe-1* ^{5} fly lines. This revealed a 5 bp deletion at the beginning of the second exon of *dGe-1-A* in the *dGe-1* ^{4} line, and a 2 kb fragment of the P element remaining at the original insertion site. The 5 bp deletion may affect the splicing of the first intron of *dGe-1*. In the *dGe-1* ^{5} mutation, a 681 bp-long deletion covering most of the *dGe-1* 5' UTR, the putative *dGe-1* promoter and a small part of 3'UTR of the upstream gene, *CG6192*, was detected. In addition, a 30 bp fragment of unknown origin was inserted into this region. The deletion of the putative promoter and the strong lethality of the *dGe-1* ^{5} mutant suggests that *dGe-1* ^{5} is one of the strongest alleles identified in this screening. Although *dGe-1* ^{4} exhibited the same lethal phase as *dGe-1* ^{5}, the large P element fragment remaining in *dGe-1* ^{4} mutant rendered prediction of the mutated gene products somewhat unclear. Therefore, because of the strong allelic strength and the relative simplicity of the *dGe-1* ^{5} deletion, *dGe-1* ^{5} was used to study the function of *dGe-1* during *Drosophila* oogenesis.

Since the *dGe-1* ^{5} mutation also removed part of the 3' UTR of *CG6192*, I performed genetic experiments to prove that the lethality of *dGe-1* ^{5} was due to a defect in *dGe-1* and not in *CG6192* function. Firstly, in complementation tests, the *dGe-1* ^{5}/ *dGe-1* ^{4}and *dGe-1* ^{5}/ *dGe-1* ^{163} trans-heterozygous combinations, in which one copy of normal *CG6192* is still present, were still lethal. This suggests that the *CG6192* gene product cannot rescue the lethality of the *dGe-1* mutant. Secondly, the lethality of *dGe-1*^{5} as well as *dGe-1* ^{4} could be rescued by a transgenic construct expressing *dGe-1* cDNA under control of the ubiquitous tubulin promoter or of sequences from the presumptive promoter region of endogenous *dGe-1*.

To test if mRNA levels of *dGe-1* were affected by the *dGe-1* ^{5} mutation, I performed RT-PCR on the total ovarian RNA from the *dGe-1* ^{5} mutant and *wild-type* flies. Since *dGe-1* ^{5} homozygous flies do not survive to adulthood, I generated the *dGe-1* ^{5} *germ-line-clone* (*GLC*) mutant ovaries in the *dGe-1*

heterozygous females using the FRT-DFS technique (see section 2.1.5). For the RT-PCR analysis, three sets of primers targeting different regions of both of the *dGe-1* transcripts were used (Figure 12A, the blue, red and green primers). For each set of primers, little - if any, amplification was detected in the *dGe-1* ^{5} sample, compared with the *wild-type* sample (Figure 12D). These results indicated, first, that *dGe-1* mRNA levels are dramatically reduced in the *dGe-1* ^{5} *GLC* ovaries and, second, that there was no abundant truncated *dGe-1* transcript is produced from sequences downstream of the deletion region.

Because of the strong reduction in *dGe-1* mRNA amounts in *dGe-1* ^{5} mutant, I speculated that the dGe-1 protein levels should also decrease. To test if it was the case, I carried out a western blot analysis of protein lysates of early embryos produced by *dGe-1* ^{5} ^{5} *GLC* females. In the *dGe-1* ^{5} mutant, a band just above the 150 kDa marker observed in the *wild-type* lysate was specifically reduced (Figure 12C). This suggests that this upper band represents dGe-1 protein on western blots, whereas that the lower band is non-specific, and that the production of dGe-1 protein is also strongly affected by the *dGe-1* ^{5} mutation.

3.3 dGe-1 protein is a P-body component in the fly germline

3.3.1 *dGe-1* is distributed in a punctate pattern in the nurse cells

The distribution of dGe-1 protein during oogenesis was revealed by immunostaining of ovaries using the anti-dGe-1 antibody. From early oogenesis onwards, dGe-1 protein could be detected in the nurse cells and the oocyte, as well as in the follicle cells (Figure 13A). Notably, in the cytoplasm of the nurse cells, the dGe-1 staining revealed a punctate distribution of the protein (Figure 13B). To exclude the possibility that this staining was due to non-specific binding of anti-dGe-1 antibody, I generated UASp-Flag:HA:dGe-1 transgenic flies (hereafter referred to as FH:dGe-1), expressed the FH:dGe-1 protein specifically in the female germline using the GAL4-UAS technique (see section 2.1.4) and examined the distribution of the exogenous HA-tagged

dGe-1 protein using an anti-HA antibody. Anti-HA immunodetection revealed that the FH:dGe-1 protein is similarly distributed in puncta in the nurse cell cytoplasm (Figure 13C), suggesting that the observed immunostaining of the endogenous dGe-1 was specific. Most importantly, the staining of dGe-1 puncta in the nurse cell was dramatically reduced in *dGe-1*$^{\Delta 5}$ *GLC* egg-chambers, whereas dGe-1 protein was still detected in the *dGe-1* ^{5} heterozygous follicle cells (Figure 13D). Interestingly, this punctate distribution of dGe-1 protein in the nurse cell was highly reminiscent of P-bodies, suggesting that in dGe-1 protein might be also a P-body component in the *Drosophila* germline.

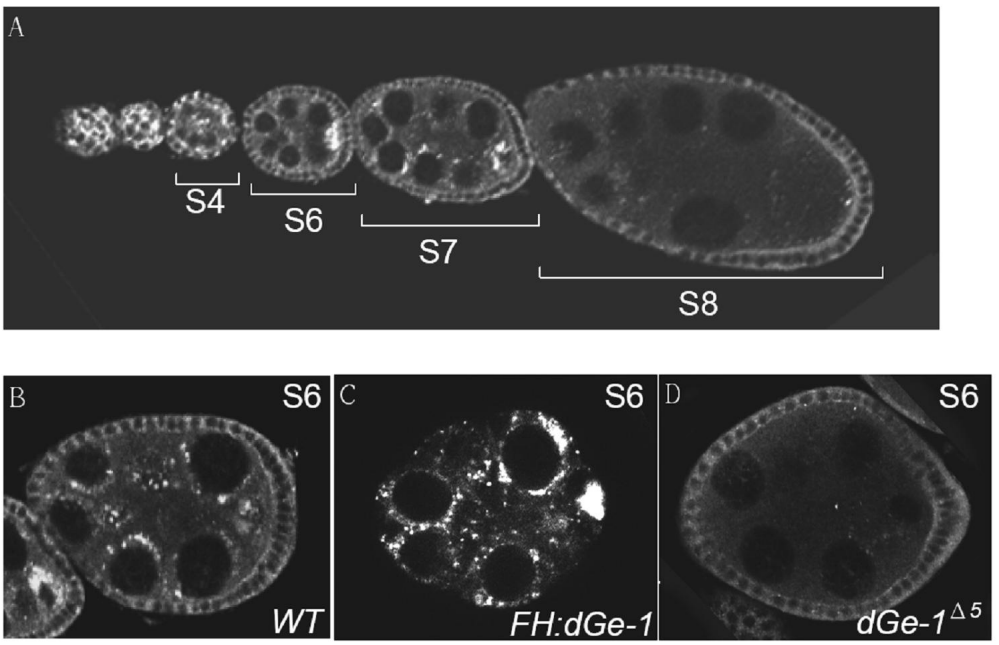

Figure 13 **The distribution of dGe-1 protein during *Drosophila* oogenesis**

(A, B, D) The distribution of dGe-1 protein was revealed by immuno-staining using anti-dGe-1 antibody. (A) An overview of dGe-1 protein distribution during oogenesis. dGe-1 protein was observed in all cell types in the *wild-type* egg-chamber, from early oogenesis onwards. (B) In the S6 egg chamber, dGe-1 protein is distributed in a punctate pattern in the cytosol of the nurse cells. (C) The FH:dGe-1 (3 copies of flag-and 3 copies of HA were fused to the N-terminus of dGe-1) was expressed in the fly germ-line using the Gal4-UAS technique. Its distribution was then revealed by anti-HA immuno-staining. Similar to the endogenous dGe-1 protein, the epitope-tagged dGe-1 showed a punctate pattern. (D) The dGe-1 staining in the nurse cells was absent from *dGe-1*$^{\Delta 5}$ *GLC* egg-chambers

3.3.2 *dGe-1* colocalizes with P-body components in the nurse cells

Although it has been shown that dGe-1 is a P-body component in cultured *Drosophila* S2 cells, so far there has been no evidence showing that this is the case *in vivo* (Eulalio et al., 2007b; Eulalio et al., 2007c). To test if it might be the case, I performed co-immunodetection in fly ovaries of dGe-1 protein and previously identified P-body components. Me31B, the *Drosophila* homologue of Dhh1, has been considered as a P-body marker in *Drosophila* (Eulalio et al., 2007b; Lin et al., 2008). In *wild-type* egg-chambers Me31B protein showed a speckled distribution in the nurse cell (Figure 14B), where it largely colocalized with dGe-1 protein (Figure 14A, C). Trailer hitch (Tral), the *Drosophila* homologue of RAP55, is also a P-body marker in the fly (Eulalio et al., 2007b). In the cytoplasm of the nurse cells, Tral protein was localized in cytoplasmic foci (Figure 14E) in which dGe-1 protein was also detected (Figure 14D, F). Moreover, colocalization of the exogenous FH:dGe-1 protein and Me31B protein was also observed (Figure 14G, H, I). It has been shown that over-expression of Dcp1 in mammalian cells can promote the P-body assembly (Fenger-Gron et al., 2005). In the fly germline, I observed a similar phenotype upon YFP:dDcp1 was expressed in the presence of the endogenous dDcp1 (Figure 14K): the YFP:dDcp1 assembled into enlarged P-body-like structures in the nurse cells, and dGe-1 protein was also detected within these strucures. (Figure 14J, L). Based on the colocalization of dGe-1 protein with three major P-body components, I conclude that dGe-1 is a P-body component in the *Drosophila* germline.

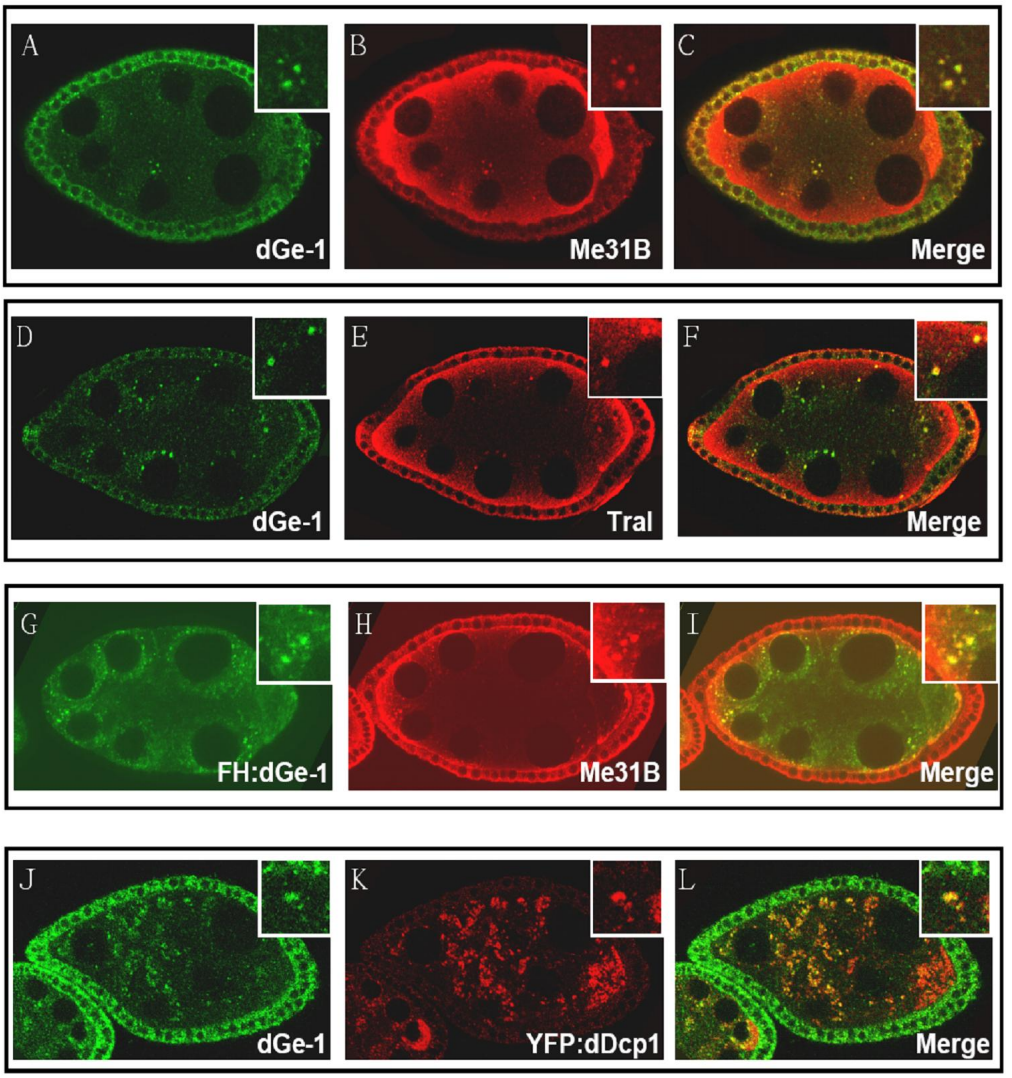

Figure 14 **dGe-1 is a P-body component in the *Drosophila* germline**

(A, D) In the cytoplasm of the nurse cells, dGe-1 protein accumulates in puncta. (B, E) Two P-body components, Me31B and Traler Hitch colocalize with dGe-1. (C, F) The merge of the dGe-1 and P-body component stainings. (G) The exogenous FH:dGe-1 protein can also be detected in Me31B-positive foci (H, I). (K) dDcp1 is another conventional P-body marker. In the nurse cells, dGe-1 staining overlaps with YFP:dDcp1 staining (J, L). Insets: a zoom-in of the dGe-1 puncta.

3.3.3 *dGe-1* associates with P-body component dGe-1 in ovaries

Having shown by colocalization that dGe-1 is a P-body component in the *Drosophila* germline, I tested whether dGe-1 might be associated with other P-body components. It has been shown that Dcp1 and Ge-1 can associate in mammalian and plant cells (Fenger-Gron et al., 2005; Xu et al., 2006). To determine if it is also the case in the *Drosophila* ovary, I examined the interaction between dDcp1 and dGe-1 by co-immunoprecipitation (Figure 15A). An ovarian extract of flies expressing YFP:dDcp1 was subjected to immunoprecipitation using anti-YFP antibody. Due to the unavailability of a suitable YFP fusion control extract, in these initial experiments a w^{1118} ovarian extract was used as the control. In the input samples, YFP was only detected in the YFP:dDcp1 lysate, not in the w^{1118} control lysate. Notably, in the input, the amount of dGe-1 protein was greater in the YFP:dDcp1 lysate than in the control lysate. This was not due to a difference in the amounts of extract loaded, because the Khc protein levels were comparable in the two samples. After the immunoprecipitation, YFP-dDcp1 was detected in the bound fraction. Interestingly, the amount of dGe-1 protein detected in the YFP-dDcp1 precipitated fraction was greater than in the control. This suggests that YFP-dDcp1 and dGe-1 may be associated with the same biochemical complex.

To test whether the association of dGe-1 with dDcp1 is RNA-dependent, I treated the ovarian lysate with RNAse A, an endonuclease that hydrolyzes single-stranded RNA, before performing immunoprecipitation (Figure 15B). It has been shown that the association between dDcp1 and Exu is RNA-dependent (Lin et al., 2006). This association was disrupted after RNAse A treatment (Figure 15B). Interestingly, the co-immunoprecipitation of dGe-1 with YFP:dDcp1 was not abolished by RNAse A treatment, suggesting that the interaction of dGe-1 with dDcp1 is not mediated by RNA.

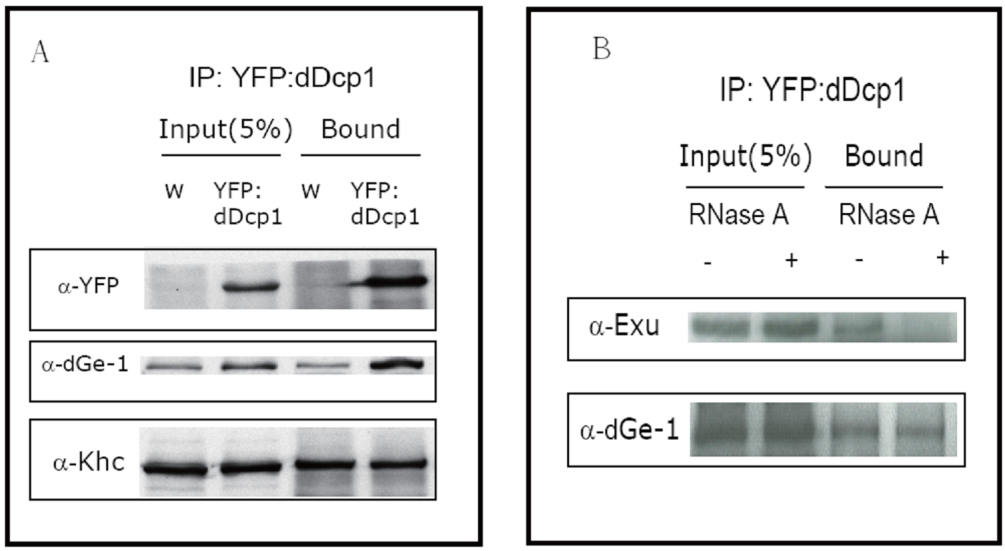

Figure 15 **dGe-1 protein associates with dDcp1**

(A) A YFP:dDcp1 ovarian extract was immunoprecipitated using an anti-YFP antibody. A *wild-type* ovarian extract was used as a control. dGe-1 protein was enriched in the YFP:dDcp1 coimmunoprecipitation. Kinesin heavy chain was used as a loading control. (B) The interaction between dGe-1 and YFP-dDcp1 is resistant the RNase treatment. The association between Exu and dDcp1, which is RNase-sensitive, was served as a control.

3.4 *dGe-1* is required for P-body formation in the *Drosophila* germline

While a requirement for Ge-1 protein in the formation of P-bodies in cells has been shown, it is still unknown if Ge-1 performs the same function *in vivo*. To address this, I examined P-body formation in the ovaries of *dGe-1* mutant flies, staining for different P-body markers. As described in section 3.2, Me31B is present in cytoplasmic foci and serves as a marker for P-bodies in the *wild-type* nurse cell (Figure 16A) (Lin et al., 2008). Interestingly, in *dGe-1* ^{5} *GLC* ovaries, the Me31B foci were dramatically reduced in number and size (Figure 16B). This suggests that dGe-1 is either required for P-body formation or for recruitment of Me31B protein to P-bodies. To distinguish between these two possibilities, I analyzed the distribution of another P-body marker, Cup,

which is a functional homologue of 4E-T (Ferraiuolo et al., 2005), was checked in *wild-type* and *dGe-1 ^{5} GLC* egg-chambers (Figure 16C, D). Similarly, the loss of dGe-1 protein resulted in a loss of the Cup-containing granules in the nurse cells of *dGe-1 ^{5} GLC* ovaries, which further confirmed the requirement of dGe-1 protein in P-body formation *in vivo*. To test if the failure in P-body formation in *dGe-1 ^{5} GLC* ovaries might be due to the reduced levels of other P-body components, I performed western blotting to evaluate Me31B and Cup protein levels in the mutant. This showed that the amount of Me31B and the Cup proteins is similar in *wild-type* and *dGe-1 ^{5} GLC* ovarian protein lysates (Figure 16E), indicating that dGe-1 does not act in P-body formation by controlling the levels of the other P-body components in the cell. Rather, these findings suggest a function of dGe-1 in P-body assembly.

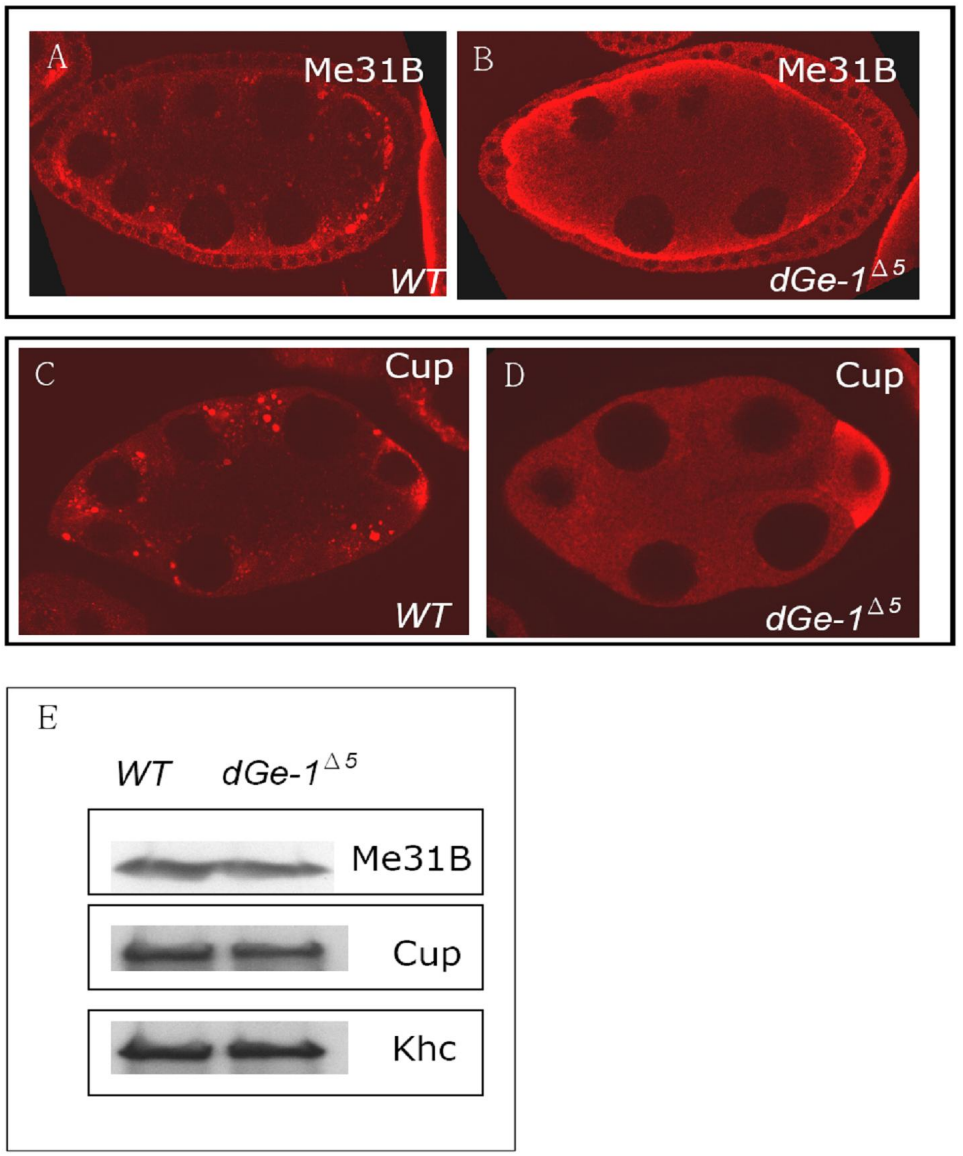

Figure 16 ***dGe-1* is required for the formation of P-bodies in the *Drosophila* germline**

(A~D) The distribution of two P-body components was detected by immuno-staining. (A) Me31B, a marker of P-bodies in the fly germline, is detected in cytoplasmic foci in a *wild-type* egg chamber. (B) In a *dGe-1*$^{\Delta 5}$ *GLC* egg-chamber, the number and size of Me31B foci were reduced. (C) Cup, a P-body component, exhibits a granular pattern in a *wild-type* egg-chamber. (D) Cup granules are absent in a *dGe-1*$^{\Delta 5}$ *GLC* egg-chamber. (E) The protein levels of Me31B and Cup were examined by western blot and were comparable in *wild-type* and *dGe-1*$^{\Delta 5}$ *GLC* ovaries. Khc: loading control.

It has been shown that over-expression of some P-body components, such as Dcp1 and Dhh1/Me31B, promotes P-body formation in mammalian cells (Fenger-Gron et al., 2005). To test whether depletion of *dGe-1* could impair this promotion of the P-body formation, I examined the distribution of YFP-tagged dDcp1 and GFP-tagged Me31B ectopically expressed in *dGe-1* ^{5} GLC egg-chambers. Consistent with my previous observation that dGe-1 is required for endogenous P-body formation, the YFP:dDcp1 and GFP-Me31B puncta were rarely observed in the *dGe-1* ^{5} *GLC* egg-chambers (Figure 17 B, E), whereas many puncta were observed in the *wild-type* egg-chambers (Figure 17A, D). However, western blot analysis showed that the YFP:dDcp1 and GFP-Me31B proteins were significantly less abundant in the *dGe-1* ^{5} *GLC* ovaries than in *wild-type* (Figure 17C, F), whereas the levels of endogenous Me31B protein were unchanged. It therefore appears that the YFP- and GFP-tags affect the stability of the two fusion proteins, which are stabilized upon incorporation into P-bodies. Consistent with the reported function of Ge-1 in cells in culture, dGe-1 protein is required for P-body formation *in vivo* in the *Drosophila* germline.

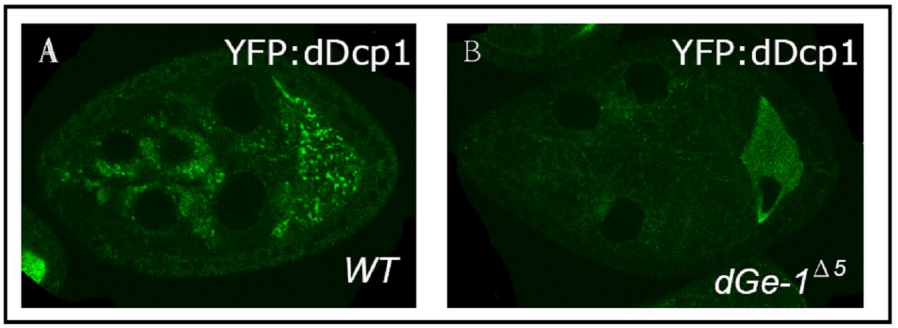
A
YFP:dDcp1
WT
B
YFP:dDcp1
dGe-1Δ5

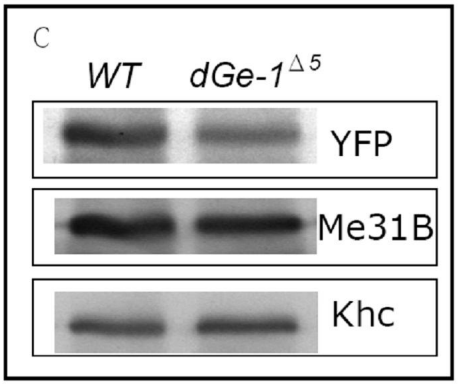
C
WT
dGe-1Δ5
YFP
Me31B
Khc

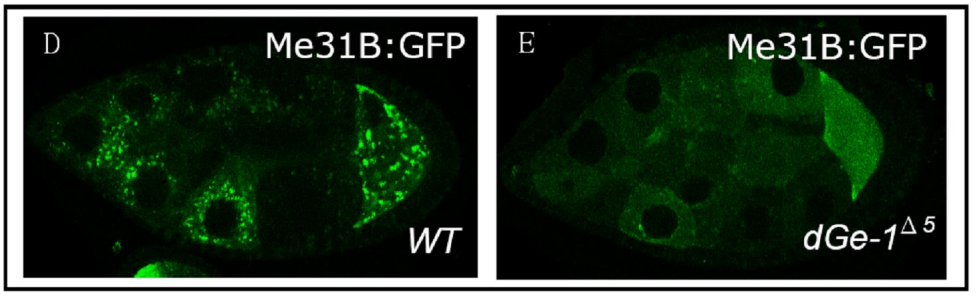
D
Me31B:GFP
WT
E
Me31B:GFP
dGe-1Δ5

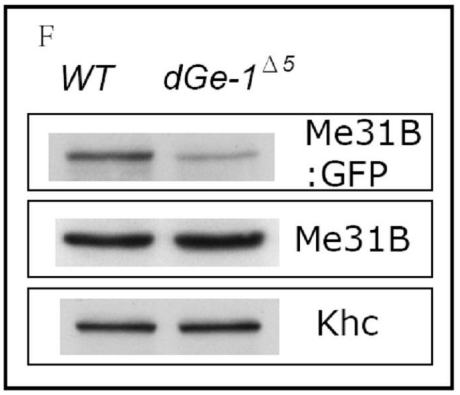
F
WT
dGe-1Δ5
Me31B
:GFP
Me31B
Khc

Figure 17 **Loss of *dGe-1* impairs the induction of the P-body-like structures by over-expressed P-body components**

(A) In a *wild-type* egg-chamber, the expression of YFP-dDcp1 protein leads to the formation of the enlarged P-body-like YFP-dDcp1 granules, as revealed by the YFP signal. (B) In *dGe-1*$^{\triangle 5}$ *GLC* egg-chambers, theYFP-dDcp1 granules are dramatically decreased in size and number. (C) Western blot analysis shows that the amount of YFP-dDcp1, detected by the anti-GFP antibody, is slightly reduced in *dGe-1*$^{\triangle 5}$ *GLC* ovarian lysate, while the amount of endogenous Me31B is unchanged. Khc: loading control. (D) The enlarged P-body-like GFP:Me31B granules in the GFP:Me31B-expressing egg-chambers was observed by the GFP signal. (E) In *dGe-1* $^{\triangle 5}$ *GLC* egg-chambers, Me31B:GFP granules were rarely observed. (F) By the western blot analysis, the amount of GFP:Me31B, assessed by anti-GFP antibody, was significantly reduced in *dGe-1*$^{\triangle 5}$ *GLC* ovarian lysate, whereas the amount of endogenous Me31B was unchanged. Khc: loading control.

3.5 *dGe-1* is involved in posterior patterning of the embryo

Given that several P-body components are also involved in *osk* mRNA regulation and that *dGe-1* is an essential component required for P-body formation in the fly germline, I was curious to know if *dGe-1* might also be involved in *osk* mRNA localization and/or translation control. It has been shown that posterior localization of *osk* mRNA and the local expression of Osk protein in the oocyte are crucial for development of the abdomen and germline in the embryo (see section 1.3.3). Characteristic of the emb ryonic abdomen are eight repetitive abdominal segments that can be directly visualized as stripes of denticles – so-called “denticle belts” – that form on the ventral side, in the posterior two-thirds of the embryo (Figure 5A,18A, B). The appearance of the abdominal denticle belts can serve as a read-out of the degree of normalcy of the abdominal patterning process, which depends on the amount of Osk protein at the posterior pole of the oocyte.

For the analysis of the abdominal cuticle patterns of the embr yos developed from *dGe-1* GLC, I classified the observed “posterior group” phenotypes (see introduction) in two categories: (1) the “strong” posterior group phenotype, in

which the abdominal denticle belts or, in other words, the abdomen were completely missing (Figure 18E, F) and (2) the “weak” posterior phenotype, in which at least one abdominal denticle belt was missing, indicating that part of the abdomen failed to develop (Figure 18C, D).

As expected, more than 90% of the embryos derived from *wild-type* mother hatched and showed normal abdominal development; a few eggs failed to hatch (9%) and had no cuticle whatsoever, suggesting they were unfertilized (Table 2). Importantly, none of the progeny of *wild-type* females exhibited a posterior group phenotype. Similarly, no posterior group phenotype and a very low unhatched rate were observed among the embryos produced by *dGe-1* ^{5} heterozygous mothers. In contrast, 45% of the embryos developed from *dGe-1* ^{5} clones failed to hatch, indicating that maternal *dGe-1* plays a role during embryogenesis. Notably, a small proportion of the unhatched embryos exhibited different degrees of posterior patterning defects. Around 3% of *dGe-1* ^{5} mutant embryos displayed a weak posterior group phenotype, and about 1% showed a strong phenotype, whereas no ectopic abdominal structures or obvious defects in the head formation were observed. Most importantly, the defects in posterior patterning as well as the lethality of the embryos developed from *dGe-1* ^{5} clones could be rescued by expressing dGe-1 protein in the maternal germline, demonstrating that these phenotypes displayed by *dGe-1* ^{5} embryos is specifically due to the loss of *dGe-1*.

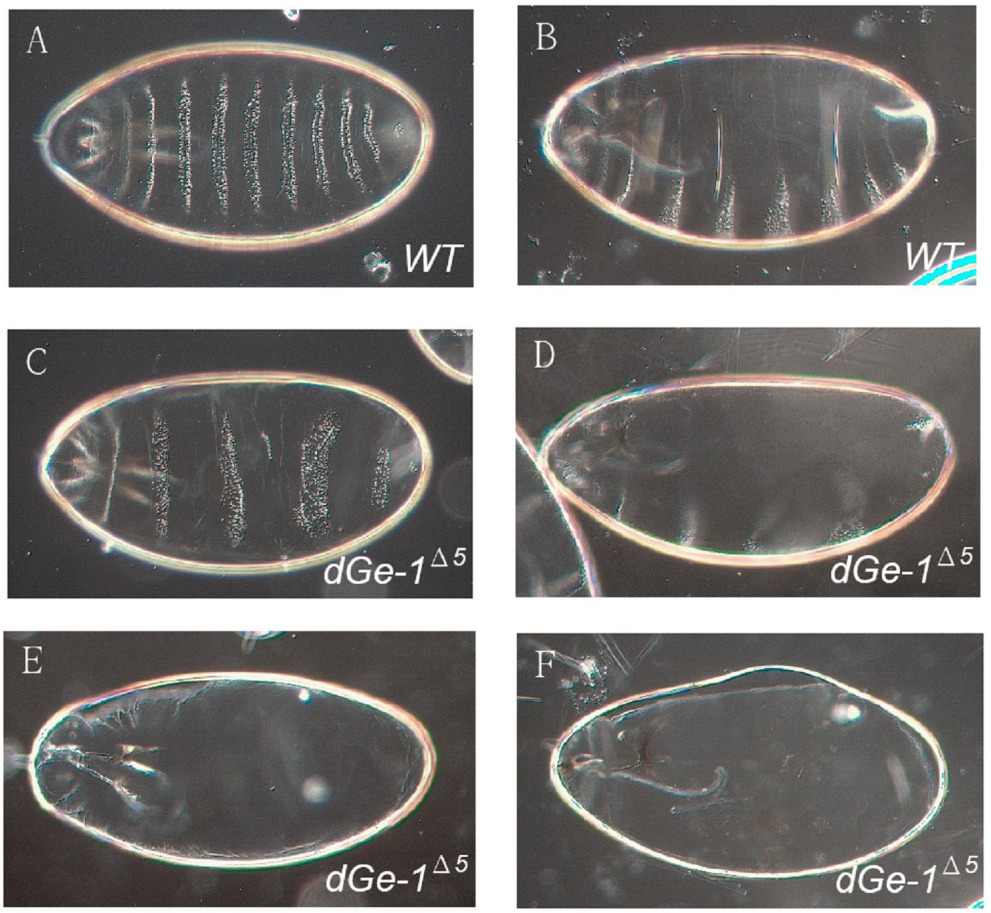

Figure 18 **Loss of maternal *dGe-1* affects the development of posterior structures in the embryo**

Embryo cuticle preparations. Embryos are oriented anterior to the left, posterior to the right.(A, C, E) A ventral view of the embryos. (B, D, F) A lateral view of the embryos. (A, B) In a *wild-type* embryo, the posterior structures represented by the abdominal denticle belts are clearly visible along the ventral side. (C,D) In some of the mutant embryos derived from the *dGe-1*$^{\Delta 5}$ *GLC*, the ventral denticle belts are not completely formed, indicating that the development of posterior structures was partially defective. (E,F) In extreme cases, the abdominal denticle belts were entirely absent from *dGe-1*$^{\Delta 5}$ GLC mutant embryos, suggesting a failure in posterior patterning.

Table 2 **Loss of maternal *dGe-1* affects the embryonic posterior patterning**

The statistics of different embryonic phenotypes in the *dGe-1*$^{\Delta 5}$ mutant. Unhatched: all kinds of unhatched eggs. No cuticle: the unhatched eggs with no cuticle formation, which is probably due to unfertilization. Weak: the weak posterior phenotype. Strong: strong posterior group phenotype.

Genotype	Unhatched	No cuticle	Posterior group		n
			Weak	Strong	
+/+	8.96%	8.44%	0%	0%	569
dGe-1$^{\Delta 5}$/+	5.60%	3.69%	0%	0%	732
dGe-1$^{\Delta 5}$/ *dGe-1*$^{\Delta 5}$	45.23%	15.59%	3.18%	0.78%	1289
dGe-1$^{\Delta 5}$/ *dGe-1*$^{\Delta 5}$, *tub:dGe-1*	24.33%	16.08%	0%	0%	970

3.6 *dGe-1* is involved in *osk* mRNA localization

3.6.1 Loss of *dGe-1* affects Osk protein and *osk* mRNA localization

The mild posterior patterning defects observed among *dGe-1* ^{5} GLC embryos suggested a possible involvement of *dGe*-1 in *osk* mRNA localization and/ or Osk protein production. Therefore, I examined the distribution of Osk protein in stage 10 (S10) *wild-type* and *dGe-1* ^{5} GLC mutant oocytes. In the *wild-type* egg-chambers at S10, Osk protein accumulated as a crescent at the posterior pole of the oocyte (Figure 19A). Consistent with the embryonic posterior patterning defects of *dGe-1* mutant embryos, *dGe-1* ^{5} mutant oocytes exhibited abnormal Osk protein localization to different degrees (Figure 19D, G, J). In addition, no ectopic Osk protein was detected in the *dGe-1* ^{5} mutant oocytes (Figure 19D, G, J), consistent with the observation that none of the *dGe-1* ^{5} mutant embryos showed ectopic abdomen formation. To test whether the defect in Osk protein localization was due to *osk* mRNA mislocalization, the distribution of *osk* mRNA in the *dGe-1* ^{5} mutant oocytes was also examined. Similar to Osk protein, *osk* mRNA also exhibited different degrees of

mislocalization (Figure 19B, E, H, K). For analysis, the *osk* mRNA localization defects were arbitrarily assigned into four categories: normal, dispersed, weak and absent. While 97% (n=47) of the S10 *wild-type* oocytes exhibited normal *osk* mRNA localization, only 79% (n=39) of the *dGe-1* ^{5} mutant oocytes showed proper posterior *osk* mRNA localization (Figure 21B). Interestingly, in the S10 *dGe-1* ^{5} GLC oocytes, the localization of *osk* mRNA was highly correlated to that of Osk protein (Figure 19F, I, L), in some instances the dispersed localization of Osk protein overlapping completely with that of *osk* mRNA. This suggests that the defects in the Osk protein localization in the *dGe-1* ^{5} mutant oocytes results from mislocalization of *osk* mRNA.

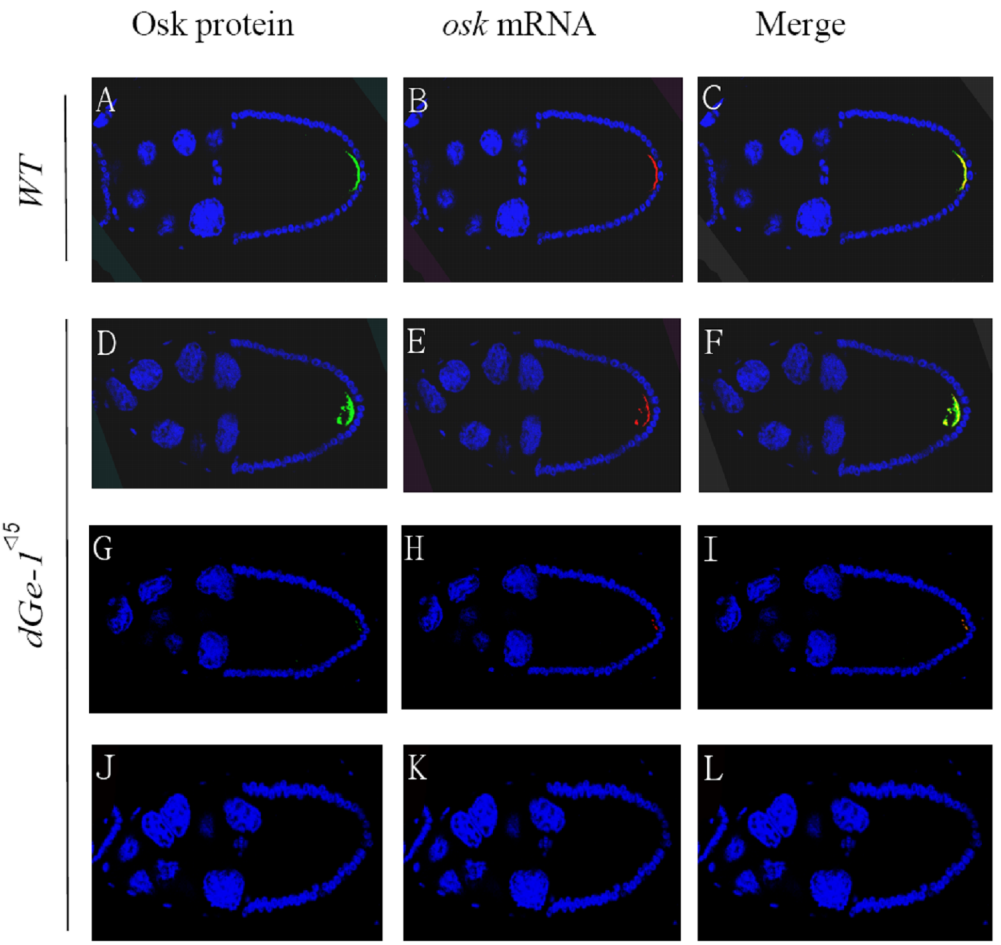

Figure 19 **Loss of *dGe-1* affects posterior localization of *osk* mRNA and Osk protein in the S10 oocytes**

Double stainings by fluorescent RNA *in situ* hybridization coupled with immunofluorescent detection of protein reveals the distributions of Osk protein and *osk* mRNA simultaneously. (A) Osk protein (green) and (B) *osk* mRNA (red) are both detected in a posterior crescent at the posterior pole of a S10 *wild-type* oocyte. (D-L) Examples of the aberrant distributions of Osk protein and *osk* mRNA observed in *dGe-1*$^{\Delta 5}$ *GLC* egg chambers. (C, F, I, L) Merge of Osk protein and *osk* mRNA signals. Blue: DAPI.

The mislocalization of *osk* mRNA in the S10 *dGe-1* ^{5} oocytes could be due to defects in its transport or in its anchoring. To distinguish between these two possibilities, the distribution of *osk* mRNA was examined in S9 oocytes, in which the transport mechanism is primarily responsible for posterior

localization of *osk* mRNA, and the requirement for an anchoring mechanism is not yet apparent. Indeed, as in the case of S10 oocytes, the S9 *dGe-1* ^{5} GLC oocytes exhibited a variety of *osk* mRNA localization defects (Figure 20B, C, D). In contrast to wild-type S9 egg-chambers, among which 83% (n=135) showed normal *osk* mRNA localization, only 67% (n=71) of the *dGe-1* ^{5} showed *osk* mRNA normally localized at the posterior pole (Figure 21A). These findings therefore suggest a role of *dGe-1* in *osk* mRNA transport.

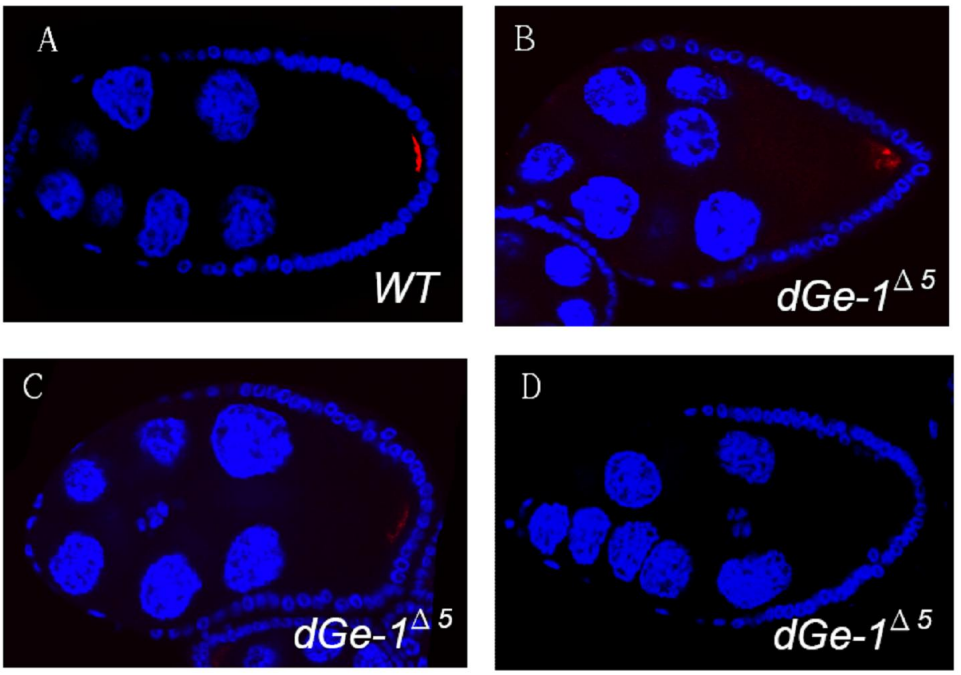

Figure 20 **Loss of *dGe-1* affects the posterior localization of *osk* mRNA in the S9 oocytes**

(A) *osk* mRNA (red) is posteriorly localized in an S9 *wild-type* oocyte. (B, C, D) Different *osk* mRNA mislocalization phenotypes are observed in *dGe-1*$^{\Delta 5}$ *GLC* egg-chambers. (B) Dispersed *osk* mRNA localization. (C) Weak posterior localization. (D) No posterior signal detected. Blue: DAPI.

3.6.2 *dGe-1* interacts genetically with other genes involved in *osk* mRNA localization and in posterior patterning

To confirm a role of *dGe*-1 in *osk* mRNA localization, I performed genetic interaction tests between *dGe-1* and other genes involved in *osk* mRNA

transport. I first examined their interactions in posterior patterning of the embryo. Kinesin heavy chain (Khc) is a key component of the kinesin -1 motor complex and is essential for *osk* mRNA transport (Brendza et al., 2000b). Although removing one copy of *khc* in *dGe-1* ^{5} homozygous mutant GLC increased the rate of unhatched embryos from 45% to nearly 80%, these was no obvious enhancement of defects in posterior patterning (Table 3). This suggests either that *dGe-1* and *Khc* are not involved in the same aspect of the *osk* mRNA transport process, or that the Khc protein is not a limiting component in the germline. dDcp1, a component of *osk* mRNPs, is required for *osk* mRNA localization (Lin et al., 2006). Removal of one copy of *dDcp1* in *dGe-1* ^{5} mutant GLC not only increased the rate of unhatched embryos - from 45% to 70%, but also significantly increased the number of embryos showing a strong posterior group phenotype - from less than 1% to greater than 6%, as well as the overall proportion of embryos with some sort of posterior group phenotype - from 4% to12% (Table 3). Barentsz (Btz), one of the core components of the EJC, is required for *osk* mRNA localization (van Eeden et al., 2001). Removal of one copy of *btz* in *dGe-1* ^{5} GLC also dramatically increased the penetrance of the strong and the weak posterior group phenotypes to 16% and 13%, respectively in the embryos (Table 3). Stau is a RNA binding protein and colocalizes with *osk* mRNA in the oocyte, suggesting that it is a *osk* RNP component (St Johnston et al., 1991). In addition to a high unhatched rate, more than 30% of the embryos developing from *stau*^{D3}*/+; dGe-1* ^{5} */ dGe-1* ^{5} GLC oocytes showed some degree of abdominal structure deletion (Table 3). Hence, similar to *dDcp1* and *btz, stau* also showed a strong genetic interaction with *dGe-1*. In addition, the high penetrance of the posterior group phenotype in these experiments was not merely due to the halving of the dose of the known *osk* mRNP components, this did not cause abdominal patterning defects in embryos produced by *dGe-1* heterozygous females (Table 3). Furthermore, the strong genetic interaction in posterior patterning between *dGe-1* and *stau* could be suppressed by expression of a *dGe-1* cDNA in *stau*^{D3}*/+; dGe-1* ^{5} */ dGe-1* ^{5} ovaries (Table 3). Taken together, these results indicate that dGe-1 cooperates with *osk* mRNP components in posterior patterning of the embryo.

Table 3 **Genetic interaction between *dGe-1* and genes involved in *osk* mRNA localization**

The statistics of different embryonic phenotypes in the different genetic backgrounds. Unhatched: all kinds of unhatched eggs. No cuticle: the unhatched eggs with no cuticle formation, which is probably due to unfertilization. Weak: the weak posterior phenotype. Strong: strong posterior group phenotype.

Genotype	Unhatched	No cuticle	Posterior group		n
			Weak	Strong	
$dGe\text{-}1^{\Delta 5}/dGe\text{-}1^{\Delta 5}$	45.23%	15.59%	3.18%	0.78%	1289
$dGe\text{-}1^{\Delta 5},khc^{27}/dGe\text{-}1^{\Delta 5},+$	79.05%	33.69%	3.33%	1.90%	840
$dGe\text{-}1^{\Delta 5},dDcp1^{b53}/dGe\text{-}1^{\Delta 5},+$	70.99%	28.33%	6.24%	6.24%	593
$dGe\text{-}1^{\Delta 5}/dGe\text{-}1^{\Delta 5};btz^{2}/+$	98.82%	38.42%	12.77%	15.96%	846
$dGe\text{-}1^{\Delta 5},stau^{D3}/dGe\text{-}1^{\Delta 5},+$	73.55%	23.42%	22.59%	10.19%	363
$dGe\text{-}1^{\Delta 5},stau^{D3}/dGe\text{-}1^{\Delta 5},+$; *tub:dGe-1/+*	39.40%	21.20%	1.25%	0%	802
$dGe\text{-}1^{\Delta 5},dDcp1^{b53}/+,+$	N.D.	N.D.	0%	0%	>500
$dGe\text{-}1^{\Delta 5}/+;btz^{2}/+$	5.24%	1.75%	0%	0%	630
$dGe\text{-}1^{\Delta 5}, stau^{D3}/+,+$	N.D.	N.D.	0%	0%	>500

A genetic interaction between *dGe-1* and components of *osk* mRNPs was also observed regarding *osk* mRNA localization. The removal of one copy of *dDcp1* in S9 and S10 *dGe-1* ^{5} mutant oocytes reduced the percentage of oocytes with normal *osk* mRNA localization from 67% to 48% and from 79% to 70%, respectively (Figure 21A, B). When one copy of *stau* was removed from the *dGe-1* ^{5} *GLC* mutant oocytes, normal *osk* localization at S9 and S10 oocytes was further decreased to 35% and 48%, respectively (Figure 21A, B). In addition, the increase of the *osk* mislocalization phenotype in these experiments was not merely due to the halving of the dose of dDcp1 or Stau; this did not cause *osk* mRNA localization defects in *dGe-1* heterozygous oocytes (Figure 21A, B). Hence, the strong genetic interaction of *dGe-1* with *osk* mRNP components in *osk* mRNA localization and posterior patterning confirms the role of *dGe-1* in the *osk* mRNA localization. In addition it suggests that dGe-1 and *osk* mRNP components act in the same process in *osk* mRNA localization.

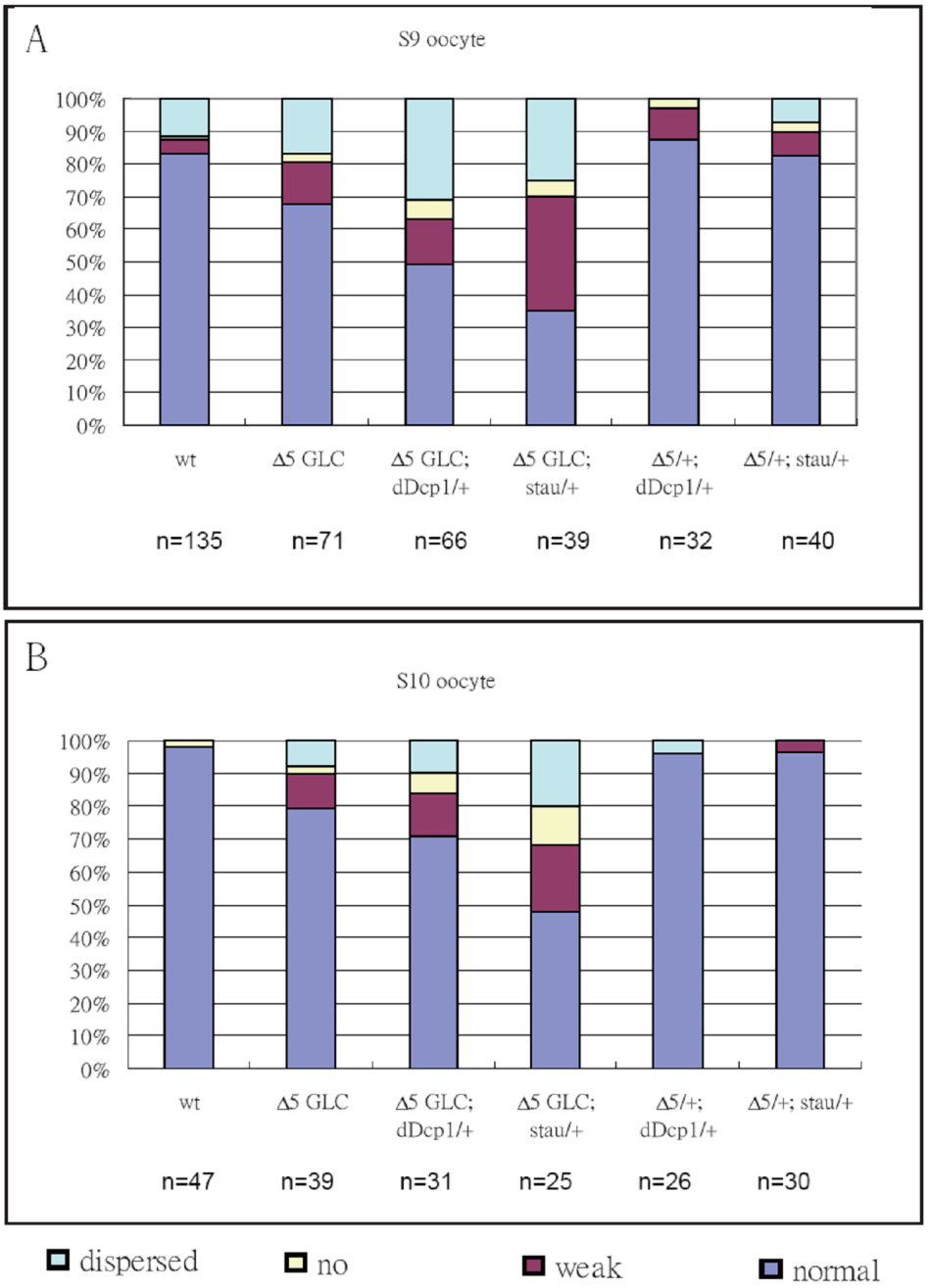

Figure 21 **The reduction in amount of *osk* mRNP components enhances the *dGe-1* mutant *osk* mRNA mislocalization phenotype**

Two diagrams show the percentages of different phenotypes of *osk* mRNA localization in S9 (A) and S10 (B) egg chambers. Cyan: dispersed localization. Purple weak posterior localization. Yellow: no posterior localization. Blue: normal posterior localization. The percentage of the oocytes showing a mislocalization of *osk* mRNA was higher in *dGe-1* mutant oocytes than in *wild-type*. The defects in *osk* mRNA localization were enhanced by decreasing *dDcp1* and *stau* gene dosage.

3.6.3 Loss of *dGe-1* does not affect the localization of *grk* and *bcd* mRNA

To test if the loss of *dGe-1* also affects the localization of other mRNAs, I also examined the distribution of *grk* and *bcd* in *dGe-1* ^{5} GLC oocytes. In *wild-type* oocytes, *grk* mRNA was localized at the anterio-dorsal corner (Figure 22A). In the *dGe-1* ^{5} mutant oocytes, its localization was not affected (Figure 22B). *bcd* mRNA was anteriorly localized in the *wild-type* oocyte (Figure 22C). Similarly, *bcd* mRNA was correctly localized at the anterior in *dGe-1* ^{5} GLC oocytes (Figure 22D). Taken together, these data show that the effect of *dGe-1* on *osk* mRNA localization is specific.

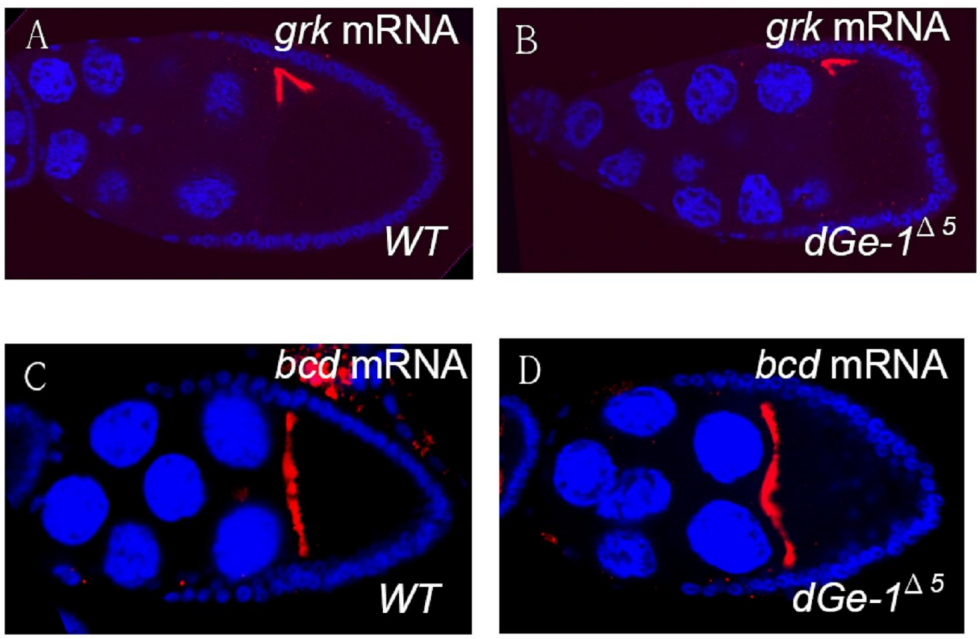

Figure 22 **Loss of *dGe-1* does not affect *gurken* or *bicoid* mRNA localization**
(A) *grk* mRNA is localized at the antero-dorsal corner of a *wild-type* oocyte. (B) In *dGe-1*$^{\Delta 5}$ mutant oocytes, *grk* mRNA distribution was not affected. (C) In a *wild-type* egg chamber, *bcd* mRNA accumulates at the anterior cortex of the oocyte. (D) The *dGe-1*$^{\Delta 5}$ mutant oocytes exhibited normal *bcd* mRNA localization.

3.7 dGe-1 protein is enriched in *osk* mRNA granules

Given that *dGe-1* is involved in *osk* mRNA localization, it was of interest to determine if dGe-1 protein associates with *osk* mRNA. During mid-oogenesis, dGe-1 protein is detected at the posterior cortex of *wild-type* oocytes (Figure 23A). Interestingly, its staining overlapped with that of Stau protein, which can serve as a reporter of the distribution of *osk* mRNA (Figure 23B, C). This suggested that dGe-1 protein and *osk* mRNA might be in the same complex. To confirm this, in collaboration with Alvar Trucco, I analyzed the relative distribution of dGe-1 protein and *osk* mRNA at the posterior pole of the oocyte, by electron microscopy, which provides a higher resolution view than confocal microscopy of the spatial localization of different molecules. At the posterior pole of *wild-type* oocytes, *osk* mRNA is distributed in electron-dense granular structures (Figure 23D). Remarkably, double-labeling for *osk* mRNA and dGe-1 protein showed that dGe-1 is enriched on the *osk* mRNA granules. Moreover, dGe-1 protein could be detected on each *osk* mRNA granule, although some dGe-1 was also detected in the cytoplasm not associated *osk* mRNA granules. The dGe-1 signal seemed to be specific, since there was no enrichment of dGe-1 protein in other cellular structures, such as yolk granules and ER. This result shows that dGe-1 is associated with *osk* mRNPs in the oocyte. To test whether this association already exists during *osk* mRNA transport, the distribution of dGe-1 protein and *osk* mRNA in the center of S9 oocytes was examined. This revealed that dGe-1 protein is also associated with *osk* mRNA granules in center of the oocyte (Figure 23E). Thus, it appears that dGe-1 is associated with the *osk* mRNPs during their transport to the posterior pole.

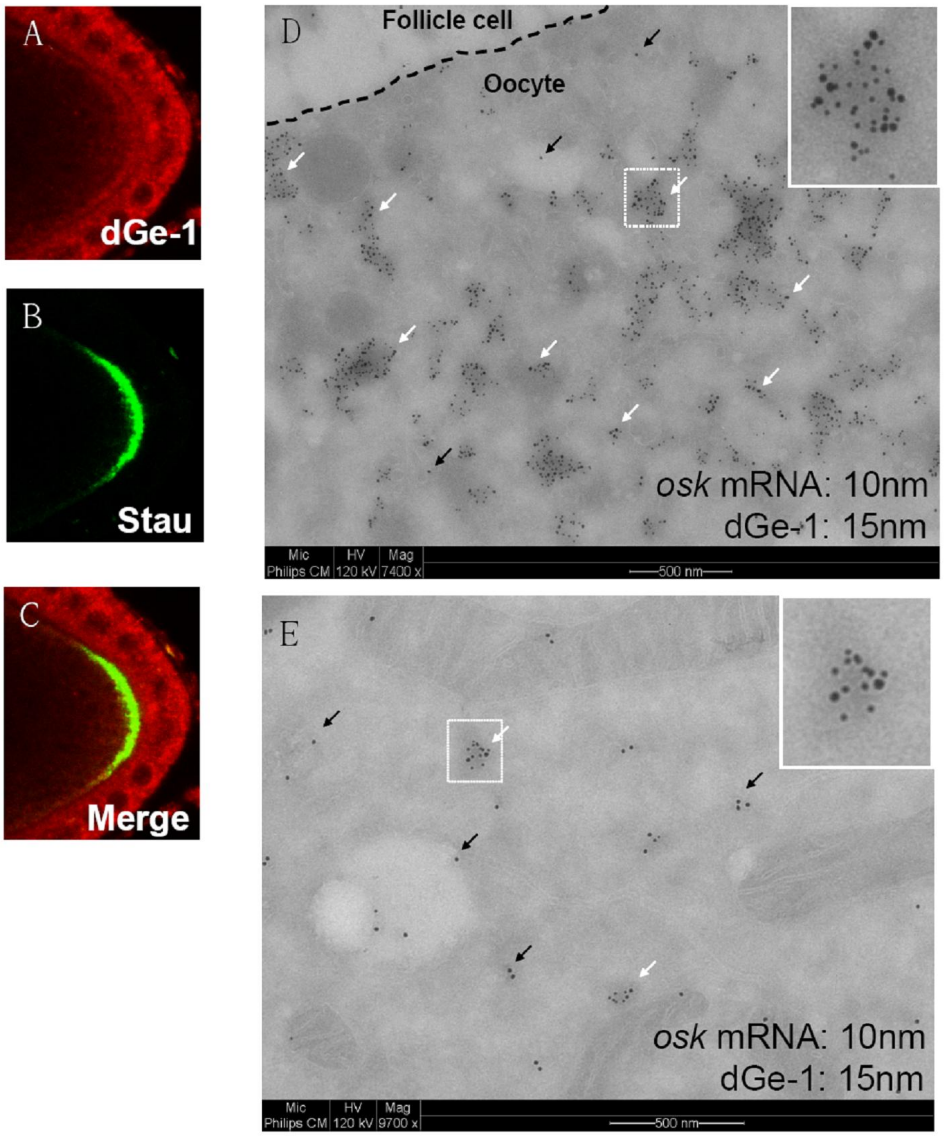

Figure 23 **dGe-1 protein is enriched in *osk* mRNA granules**

(A) dGe-1 protein is detected at the posterior cortex of the oocyte. (B) Stau protein also localizes at the posterior pole of the oocyte. (C) The merge of dGe-1 protein and Stau protein signals. (D, E) The distribution of dGe-1 protein and *osk* mRNA was examined by *in situ* hybridization coupled with electron microscopy. (D) At the posterior pole of the oocyte, *osk* mRNA (labeled with 5 nm gold) is detected in electron-dense granule structures. dGe-1 protein is labeled with 15 nm gold. The majority of detected dGe-1 protein (white arrows) was associated with *osk* mRNA granules, while some dGe-1 protein (black arrows) did not colocalize with *osk* mRNA granules. (E) In the center of the oocyte, dGe-1 protein (white arrow) was also detected associated with *osk* mRNA granules.

4. Discussion

4.1 P element remobilization as an efficient means to generate *dGe-1* mutants

In this study, two P elements GS5005 and KG05826 were used to generate *dGe-1* deletion alleles by P element imprecise excision (Figure 12A). By PCR analysis, five among 680 transposase-treated chromosomes were identified to bear deletions around the P element insertion sites. The frequency of deletion induction was 0.7 %. It is within the range of the previous reported frequencies between 0.1 % and 10 % (Greenspan, 2004). The longest deletion identified in this screening is 721 bp and the shortest one is only 5 bp (Table 1). It is also consistent with the observation of P element imprecise excision, which usually generates less than 2 kb of deletions (Greenspan, 2004). Hence, the employment of P element imprecise excision in this study provided an efficient way to create *dGe-1* deletion mutations.

4.2 dGe-1 is an obligatory P-body component *in vivo*

Knowledge of P-body biogenesis has been mostly obtained from studies on the single cell level. However, it is still unknown whether the mechanisms identified are also relevant in a multicellular context or *in vivo*. In the *Drosophila* egg-chamber, P-bodies are clearly detected in the nurse cells, as revealed by several P-body markers (Figure 14B, E and Figure 16A, C). Thus, nurse cells, combined with the powerful genetic tools in *Drosophila* provide an excellent model system to study P-body formation *in vivo*.

In this study I explored the function of dGe-1 protein in the P-body formation in *Drosophila* nurse cells. In *dGe-1* mutant egg-chambers, the Me31B and Cup granules that correspond to P-bodies were entirely absent (Figure 16B, D), indicating an absolutely requirement for dGe-1 protein in P-body formation *in vivo*. In addition, dGe-1 is a limiting factor in P-body formation in this context, as the enlarged P-body-like structures caused by over-expression of P-body

components (Fenger-Gron et al., 2005), such as YFP:Dcp1 in this study, were dramatically reduced in number and size in *dGe-1* mutant egg-chambers (Figure 17). Notably, the protein levels of the tested P-body components, Cup and Me31B, was not altered in *dGe-1* mutant ovaries (Figure 16E). Moreover, in the *wild-type* ovary dGe-1 protein colocalized with two P-body components, Me31B and Tral (Figure 14C, F). Biochemically dGe-1 associated with YFP:dDcp1 in a RNA-independent manner (Figure 15A, B). These results suggest that Ge-1 functions as a scaffold protein in P-body assembly.

A self-assembly model has been proposed for P-body formation. In yeast the Yjef-N dimerization domain of EDC3 and the prion-like Q/N-rich domain of Lsm4 have been shown to be involved in this process and have been thought to play a conserved role in higher eukaryotes (Decker et al., 2007). However, in *Drosophila* S2 cells the knockdown of Edc3 protein did not affect P-body formation (Tritschler et al., 2007). This suggests that the Yjef-N domain plays a minor role in P-body assembly in higher eukaryotes. Moreover, the Q/N-rich domain of Lsm4 is not conserved in higher eukaryotes, suggesting that another protein containing a Q/N-rich domain probably plays a similar role in these species. Interestingly, Ge-1 protein, which has no homologue in yeast, contains a Q/N-rich domain in its C-terminal region, and is absolutely required for P-body formation in cells and in the *Drosophila* germline (Figure 16, 17) (Jinek et al., 2008; Yu et al., 2005). In *Arabidopsis*, it has been shown that Ge-1 protein can oligomerize via its C-terminal domain, supporting the notion that the Q/N-rich domain might have prion-like activity (Xu et al., 2006). However, whether the Q/N-rich domain of Ge-1 protein is responsible for the assembly of P-bodies has not been shown, hence this hypothesis remains to be tested.

4.3 *dGe-1*$^{\Delta 5}$ is a strong hypomorphic allele of *dGe-1*

Although the *dGe-1*$^{\Delta 5}$ mutation strongly affects P-body formation, the penetrance of the posterior patterning defects and *osk* mislocalization in the mutant is low. This suggests a different requirement of *dGe-1* for these two cellular events. It also raised the possibility that *dGe-1*$^{\Delta 5}$ is a weak allele of *dGe-1*. However, several lines of evidence suggest that *dGe-1*$^{\Delta 5}$ is in fact a strong *dGe-1* allele. First, the region deleted in *dGe-1*$^{\Delta 5}$ goes from 448 bp

upstream to 273 bp downstream of the *dGe-1*transcription start site (TSS). Since the core promoter module of a eukaryotic gene usually surrounds the TSS, the prediction would be that the transcription regulation of *dGe-1* is seriously disrupted by the *dGe-1*$^{\Delta 5}$ mutation. Indeed, both *dGe-1* transcript and dGe-1 protein levels were dramatically reduced in *dGe-1*$^{\Delta 5}$ mutant ovaries (Figure 12C, D). In addition, the PCR amplification products using two different sets of primers targeting the 3' half of the *dGe-1* transcripts were also strongly reduced in the *dGe-1*$^{\Delta 5}$ mutant. This suggests that no truncated *dGe-1* transcripts are generated from another TSS and, thus, no truncated dGe-1 protein should be made. Taken together, these results indicate that *dGe-1*$^{\Delta 5}$ is a strong *dGe-1* allele at the molecular level. Moreover, *dGe-1*$^{\Delta 5}$ is a lethal mutation, whereas *dGe-1*$^{\Delta 56}$ was viable and *dGe-1*$^{\Delta 102}$ only semi-lethal. Hence, at the genetic level, *dGe-1*$^{\Delta 5}$ also behaved as a strong allele. Based on this genetic and molecular evidence, I conclude that the low penetrance of posterior patterning defects and *osk* mRNA mislocalization in the *dGe-1*$^{\Delta 5}$ mutant reflect the function of dGe-1 protein itself.

One possible explanation for the low penetrance of the *dGe-1* mutant phenotype is redundancy of dGe-1 protein with another protein acting at the same step in *osk* mRNA localization. Although *Drosophila* contains only one Ge-1 gene, I cannot rule out the existence of a functionally redundant protein with dGe-1 in fly. Another equally plausible explanation is that dGe-1 acts alone in a process that is not absolutely essential for *osk* mRNA localization, such as optimization of the localization process. Indeed, it is possible that, acting as a scaffold for the assembly of complexes such as P-bodies and *osk* transport RNPs, dGe-1 may simply serve to locally concentrate the proteins essential for *osk* mRNA transport, rendering *osk* RNP assembly more efficient. In the absence of dGe-1, *osk* RNP assembly process might be less efficient, yet under normal laboratory conditions function sufficiently for mRNA localization to occur and posterior patterning proceed.

4.4 dGe-1 protein is associated with *osk* mRNA and involved in *osk* mRNA localization

In this study, I have shown that the loss of maternal *dGe-1* affects posterior

patterning in the progeny embryos, shedding light on the *in vivo* function of *dGe-1* in this developmental process. The developmental defects observed in *dGe-1* embryos were further shown to be a consequence of *osk* mRNA mislocalization in *dGe-1* mutant oocytes, suggesting that, in addition to its requirement in P-body formation, *dGe-1* plays a role in *osk* mRNA localization.

Interestingly, the weak phenotypes of the embryos that developed from *dGe-1 GLC* were strongly enhanced by removal of one copy of *dDcp1*, *stau* or *btz*, each of which encodes a component of *osk* mRNPs and is involved in *osk* mRNA localization. These genetic interactions further support a function of dGe-1 in *osk* mRNA localization. Also, these genetic data suggest that dGe-1 may act together with these *osk* RNP components at same step in the mRNA localization pathway. The genetic interactions also reveal that, in the *osk* localization process, dDcp1, Stau and Btz are factors that become limiting in the absence of dGe-1. Finally, our *in situ* EM data suggest that dGe-1 protein is also a component of *osk* mRNPs, as dGe-1 protein was enriched in *osk* mRNA granules in the centre, as well as at the posterior pole of the *wild-type* oocytes. Therefore it is likely that dGe-1 protein plays a direct role in *osk* mRNA localization.

Given that dGe-1 protein is required for P-body formation, an intriguing question is whether dGe-1 protein is involved in the assembly of the *osk* granules and thereby contributes to *osk* mRNA localization. If this were the case, one explanation for the observed genetic interaction of *dGe-1* with other *osk* mRNP components might be that reduction of the level of *osk* mRNP components reduces or mildly impairs the formation of individual *osk* mRNPs, and that loss of dGe-1 protein interferes with the assembly of *osk* RNPs into larger, more highly motile transport granules. When the formation of these two degrees of *osk* mRNA structure is simultaneously impaired, the localization of *osk* mRNA would be more strongly affected. This model would add one more layer of regulation to *osk* mRNA localization. It will be interesting and important to determine if the formation of *osk* mRNA granules is disrupted in *dGe-1* mutant oocytes.

4.5 An implication on the function of P-bodies

It has been shown that P-body formation requires Ge-1 protein and the disruption of P-body formation has no obvious effect on mRNA decay and translation repression (Eulalio et al., 2007b). It is interesting to note that the loss of *dGe-1* in the fly oocyte only has a mild effect on *osk* mRNA localization; however, further reduction of *osk* mRNP components results in a strong *osk* mRNA mislocalization phenotype. It seems that under normal conditions, dGe-1 protein is not crucial for *osk* mRNA localization. However, when the *osk* mRNA localization machinery is rendered somewhat fragile, dGe-1's role becomes significant. Overall, this behavior suggests that the function of dGe-1 is to maintain the robustness of the whole system. It would therefore be interesting to test if this is also the case for the function of P-bodies in mRNA decay and translation repression. When the machineries mediating mRNA degradation and translation repression are damaged by a reduction in amount of some of their components, does a requirement for Ge-1 become apparent – suggesting a function of P-bodies in these processes? This would support the notion that the function of P-bodies is to concentrate mRNA degradation and translation repression to a small region within the cell to facilitate these molecular processes.

4.6 A prototype of the RNA granule

dGe-1 and several other proteins are components both of P-bodies and of *osk* mRNPs. In fact, the sharing of components is a common phenomenon among different types of RNA granules. For example, Tral, Dcp1, Dcp2, XRN1, and Me31B were detected both in the *Drosophila* neuronal granules and P-bodies (Barbee et al., 2006). In *Caenorhabditis elegans,* P granules, the maternal RNA storage granules, contain the P-body markers CGH-1/Dhh1 and CAR-1/RAP55 (Boag et al., 2008). This indicates a close relationship between different described RNA granules and suggests the existence of a prototype granule that consists of the common components. By associating with additional, different proteins, individual RNA granules would develop their specificity. It would therefore be interesting to identify the complete list of common components shared by the different RNA granules, which would be a first step towards understanding the general biology of the RNA granules.

In addition, the concept of the prototype RNA granule also reveals a new

strategy to study *osk* mRNA regulation. Based on the knowledge from studies of key components present in an RNA granule, one could ask if a given component plays a similar role in another granule. As shown in this study, dGe-1 is the first example of a protein initially shown be required for the P-body formation in cells that was later demonstrated to play a role in *osk* mRNA localization.

4.7 The function of *dGe-1 in vivo*

The lethality observed in some *dGe-1* alleles suggests that *dGe-1* is an essential gene that plays a crucial role in fly development. It is notable that, among the unhatched embryos derived from *dGe-1* GLC, only about 9% showed a posterior group phenotype (Table 2). This indicates that in addition to its function in posterior embryonic patterning, maternal *dGe-1* has additional functions in embryonic development. Since *dGe-1* is required for P-body formation and the function of P-bodies is completely unknown *in vivo*, it would be interesting to know if the developmental defects in the *dGe-1* mutant are due to the failure in P-body formation or other functions of *dGe-1*.

5. References

Ainger, K., Avossa, D., Morgan, F., Hill, S.J., Barry, C., Barbarese, E., and Carson, J.H. (1993). Transport and localization of exogenous myelin basic protein mRNA microinjected into oligodendrocytes. J Cell Biol *123*, 431-441.

Andrei, M.A., Ingelfinger, D., Heintzmann, R., Achsel, T., Rivera-Pomar, R., and Luhrmann, R. (2005). A role for eIF4E and eIF4E-transporter in targeting mRNPs to mammalian processing bodies. RNA *11*, 717-727.

Barbee, S.A., Estes, P.S., Cziko, A.M., Hillebrand, J., Luedeman, R.A., Coller, J.M., Johnson, N., Howlett, I.C., Geng, C., Ueda, R., *et al.* (2006). Staufen- and FMRP-containing neuronal RNPs are structurally and functionally related to somatic P bodies. Neuron *52*, 997-1009.

Besse, F., Lopez de Quinto, S., Marchand, V., Trucco, A., and Ephrussi, A. (2009). Drosophila PTB promotes formation of high-order RNP particles and represses oskar translation. Genes Dev *23*, 195-207.

Bhattacharyya, S.N., Habermacher, R., Martine, U., Closs, E.I., and Filipowicz, W. (2006). Stress-induced reversal of microRNA repression and mRNA P-body localization in human cells. Cold Spring Harb Symp Quant Biol *71*, 513-521.

Bloch, D.B., Rabkina, D., Quertermous, T., and Bloch, K.D. (1994). The immunoreactive region in a novel autoantigen contains a nuclear localization sequence. Clin Immunol Immunopathol *72*, 380-389.

Boag, P.R., Atalay, A., Robida, S., Reinke, V., and Blackwell, T.K. (2008). Protection of specific maternal messenger RNAs by the P body protein CGH-1 (Dhh1/RCK) during Caenorhabditis elegans oogenesis. J Cell Biol *182*, 543-557.

Brand, A.H., and Perrimon, N. (1993). Targeted gene expression as a means of altering cell fates and generating dominant phenotypes. Development *118*, 401-415.

Brendza, K.M., Sontag, C.A., Saxton, W.M., and Gilbert, S.P. (2000a). A kinesin mutation that uncouples motor domains and desensitizes the gamma-phosphate sensor. J Biol Chem *275*, 22187-22195.

Brendza, R.P., Serbus, L.R., Duffy, J.B., and Saxton, W.M. (2000b). A function for kinesin I in the posterior transport of oskar mRNA and Staufen protein. Science *289*, 2120-2122.

Brengues, M., Teixeira, D., and Parker, R. (2005). Movement of eukaryotic mRNAs between polysomes and cytoplasmic processing bodies. Science *310*, 486-489.

Bullock, S.L., and Ish-Horowicz, D. (2001). Conserved signals and machinery for RNA transport in Drosophila oogenesis and embryogenesis. Nature *414*, 611-616.

Cha, B.J., Koppetsch, B.S., and Theurkauf, W.E. (2001). In vivo analysis of

Drosophila bicoid mRNA localization reveals a novel microtubule-dependent axis specification pathway. Cell *106*, 35-46.

Cha, B.J., Serbus, L.R., Koppetsch, B.S., and Theurkauf, W.E. (2002). Kines in I-dependent cortical exclusion restricts pole plasm to the oocyte posterior. Nat Cell Biol *4*, 592-598.

Chekulaeva, M., Hentze, M.W., and Ephrussi, A. (2006). Bruno acts as a dual repressor of oskar translation, promoting mRNA oligomerization and formati on of silencing particles. Cell *124*, 521-533.

Cheung, H.K., Serano, T.L., and Cohen, R.S. (1992). Evidence for a highly selective RNA transport system and its role in establishing the dorsoventral axis of the Drosophila egg. Development *114*, 653-661.

Cho, P.F., Poulin, F., Cho-Park, Y.A., Cho-Park, I.B., Chicoine, J.D., Lasko, P., and Sonenberg, N. (2005). A new paradigm for translational control: inhibition via 5' -3' mRNA tethering by Bicoid and the eIF4E cognate 4EHP. Cell *121*, 411-423.

Chou, T.B., and Perrimon, N. (1996). The autosomal FLP-DFS technique for generating germline mosaics in Drosophila melanogaster. Genetics *144*, 1673-1679.

Clark, A., Meignin, C., and Davis, I. (2007). A Dynein-dependent shortcut rapidly delivers axis determination transcripts into the Drosophila oocyte. Development *134*, 1955-1965.

Clark, I., Giniger, E., Ruohola-Baker, H., Jan, L.Y., and Jan, Y.N. (1994). Transient posterior localization of a kinesin fusion protein reflects anteroposterior polarity of the Drosophila oocyte. Curr Biol *4*, 289-300.

Coller, J.M., Tucker, M., Sheth, U., Valencia-Sanchez, M.A., and Parker, R. (2001). The DEAD box helicase, Dhh1p, functions in mRNA decapping and interacts with both the decapping and deadenylase complexes. RNA *7*, 1717-1727.

Condeelis, J., Singer, R.H., and Segall, J.E. (2005). The great escape: when cancer cells hijack the genes for chemotaxis and motility. Annu Rev Cell Dev Biol *21*, 695-718.

Cougot, N., Babajko, S., and Seraphin, B. (2004). Cytoplasmic foci are sites of mRNA decay in human cells. J Cell Biol *165*, 31-40.

Coutelis, J.B., and Ephrussi, A. (2007). Rab6 mediates membrane organization and determinant localization during Drosophila oogenesis. Development *134*, 1419-1430.

Decker, C.J., Teixeira, D., and Parker, R. (2007). Edc3p and a glutamine/asparagine-rich domain of Lsm4p function in processing body assembly in Saccharomyces cerevisiae. J Cell Biol *179*, 437-449.

Delanoue, R., Herpers, B., Soetaert, J., Davis, I., and Rabouille, C. (2007). Drosophila Squid/hnRNP helps Dynein switch from a gurken mRNA transport motor to an ultrastructural static anchor in sponge bodies. Dev Cell *13*, 523-538.

Ding, D., Parkhurst, S.M., Halsell, S.R., and Lipshitz, H.D. (1993). Dynamic Hsp83 RNA localization during Drosophila oogenesis and embryog enesis. Mol Cell Biol *13*, 3773-3781.

Dreyfuss, G., Kim, V.N., and Kataoka, N. (2002). Messenger -RNA-binding proteins and the messages they carry. Nat Rev Mol Cell Biol *3*, 195-205.

Driever, W., and Nusslein -Volhard, C. (1989). The bicoid protein is a positi ve regulator of hunchback transcription in the early Drosophila embryo. Nature *337*, 138-143.

Ephrussi, A., Dickinson, L.K., and Lehmann, R. (1991). Oskar organizes the germ plasm and directs localization of the posterior determinant nanos. Cell *66*, 37-50.

Ephrussi, A., and Lehmann, R. (1992). Induction of germ cell formation by oskar. Nature *358*, 387-392.

Ephrussi, A., and St Johnston, D. (2004). Seeing is believing: the bicoid morphogen gradient matures. Cell *116*, 143-152.

Eulalio, A., Behm -Ansmant, I., and Izaurralde, E. (2007a). P bodies: at the crossroads of post-transcriptional pathways. Nat Rev Mol Cell Biol *8*, 9-22.

Eulalio, A., Behm -Ansmant, I., Schweizer, D., and Izaurralde, E. (2007b). P -body formation is a consequence, not the cause, of RNA -mediated gene silencing. Mol Cell Biol *27*, 3970-3981.

Eulalio, A., Rehwinkel, J., Stricker, M., Huntzinger, E., Yang, S.F., Doerks, T., Dorner, S., Bork, P., Boutros, M., and Izaurralde, E. (2007c). Target -specific requirements for enhancers of decapping in miRN A-mediated gene silencing. Genes Dev *21*, 2558-2570.

Fenger-Gron, M., Fillman, C., Norrild, B., and Lykke -Andersen, J. (2005). Multiple processing body factors and the ARE binding protein TTP activate mRNA decapping. Mol Cell *20*, 905-915.

Ferraiuolo, M.A., Basak, S., Dostie, J., Murray, E.L., Schoenberg, D.R., and Sonenberg, N. (2005). A role for the eIF4E -binding protein 4E -T in P-body formation and mRNA decay. J Cell Biol *170*, 913-924.

Fillman, C., and Lykke -Andersen, J. (2005). RNA decapping inside and ou tside of processing bodies. Curr Opin Cell Biol *17*, 326-331.

Forrest, K.M., and Gavis, E.R. (2003). Live imaging of endogenous RNA reveals a diffusion and entrapment mechanism for nanos mRNA localization in Drosophila. Curr Biol *13*, 1159-1168.

Franks, T.M., and Lykke -Andersen, J. (2008). The control of mRNA decapping and P-body formation. Mol Cell *32*, 605-615.

Gallo, C.M., Munro, E., Rasoloson, D., Merritt, C., and Seydoux, G. (2008). Processing bodies and germ granules are distinct RNA granules that intera ct in C.

elegans embryos. Dev Biol *323*, 76-87.
Giniger, E., Varnum, S.M., and Ptashne, M. (1985). Specific DNA binding of GAL4, a positive regulatory protein of yeast. Cell *40*, 767-774.
Glotzer, J.B., Saffrich, R., Glotzer, M., and Ephrussi, A. (1997). Cytoplasmic flows localize injected oskar RNA in Drosophila oocytes. Curr Biol *7*, 326-337.
Golic, K.G. (1991). Site-specific recombination between homologous chromosomes in Drosophila. Science *252*, 958-961.
Greenspan, R.J. (2004). Fly pushing : the theory and practice of Drosophila genetics, 2nd edn (Cold Spring Harbor, N.Y., Cold Spring Harbor Laboratory Press).
Hachet, O., and Ephrussi, A. (2001). Drosophila Y14 shuttles to the posterior of the oocyte and is required for oskar mRNA transport. Curr Biol *11*, 1666-1674.
Hachet, O., and Ephrussi, A. (2004). Splicing of oskar RNA in the nucleus is coupled to its cytoplasmic localization. Nature *428*, 959-963.
Hacker, U., and Perrimon, N. (1998). DRhoGEF2 encodes a member of the Dbl family of oncogenes and controls cell shape changes during gastrulation in Drosophila. Genes Dev *12*, 274-284.
Huynh, J.R., Munro, T.P., Smith-Litiere, K., Lepesant, J.A., and St Johnston, D. (2004). The Drosophila hnRNPA/B homolog, Hrp48, is specifically required for a distinct step in osk mRNA localization. Dev Cell *6*, 625-635.
Huynh, J.R., and St Johnston, D. (2004). The origin of asymmetry: early polarisation of the Drosophila germline cyst and oocyte. Curr Biol *14*, R438-449.
Ingelfinger, D., Arndt-Jovin, D.J., Luhrmann, R., and Achsel, T. (2002). The human LSm1-7 proteins colocalize with the mRNA-degrading enzymes Dcp1/2 and Xrnl in distinct cytoplasmic foci. RNA *8*, 1489-1501.
Jansen, R.P. (2001). mRNA localization: message on the move. Nat Rev Mol Cell Biol *2*, 247-256.
Jinek, M., Eulalio, A., Lingel, A., Helms, S., Conti, E., and Izaurralde, E. (2008). The C-terminal region of Ge-1 presents conserved structural features required for P-body localization. RNA *14*, 1991-1998.
Johnstone, O., and Lasko, P. (2001). Translational regulation and RNA localization in Drosophila oocytes and embryos. Annu Rev Genet *35*, 365-406.
Kim-Ha, J., Kerr, K., and Macdonald, P.M. (1995). Translational regulation of oskar mRNA by bruno, an ovarian RNA-binding protein, is essential. Cell *81*, 403-412.
Kim-Ha, J., Smith, J.L., and Macdonald, P.M. (1991). oskar mRNA is localized to the posterior pole of the Drosophila oocyte. Cell *66*, 23-35.
Kim-Ha, J., Webster, P.J., Smith, J.L., and Macdonald, P.M. (1993). Multiple RNA regulatory elements mediate distinct steps in localization of oskar mRNA. Development *119*, 169-178.

King, R.C. (1970). The meiotic behavior of the Drosophila oocyte. Int Rev Cytol *28*, 125-168.

Lange, S., Katayama, Y., Schmid, M., Burkacky, O., Brauchle, C., Lamb, D.C., and Jansen, R.P. (2008). Simultaneous transport of different localized mRNA species revealed by live-cell imaging. Traffic *9*, 1256-1267.

Le Hir, H., Izaurralde, E., Maquat, L.E., and Moore, M.J. (2000). The spliceosome deposits multiple proteins 20-24 nucleotides upstream of mRNA exon-exon junctions. EMBO J *19*, 6860-6869.

Lecuyer, E., Yoshida, H., Parthasarathy, N., Alm, C., Babak, T., Cerovina, T., Hughes, T.R., Tomancak, P., and Krause, H.M. (2007). Global analysis of mRNA localization reveals a prominent role in organizing cellular architecture and function. Cell *131*, 174-187.

Lehmann, R., and Frohnhofer, H.G. (1989). Segmental polarity and identity in the abdomen of Drosophila is controlled by the relative position of gap gene expression. Development *107 Suppl*, 21-29.

Lehmann, R., and Nusslein-Volhard, C. (1986). Abdominal segmentation, pole cell formation, and embryonic polarity require the localized activity of oskar, a maternal gene in Drosophila. Cell *47*, 141-152.

Li, D., and Roberts, R. (2001). WD-repeat proteins: structure characteristics, biological function, and their involvement in human diseases. Cell Mol Life Sci *58*, 2085-2097.

Lin, A.C., and Holt, C.E. (2007). Local translation and directional steering in axons. EMBO J *26*, 3729-3736.

Lin, M.D., Fan, S.J., Hsu, W.S., and Chou, T.B. (2006). Drosophila decapping protein 1, dDcp1, is a component of the oskar mRNP complex and directs its posterior localization in the oocyte. Dev Cell *10*, 601-613.

Lin, M.D., Jiao, X., Grima, D., Newbury, S.F., Kiledjian, M., and Chou, T.B. (2008). Drosophila processing bodies in oogenesis. Dev Biol *322*, 276-288.

Liu, J., Valencia-Sanchez, M.A., Hannon, G.J., and Parker, R. (2005). MicroRNA-dependent localization of targeted mRNAs to mammalian P-bodies. Nat Cell Biol *7*, 719-723.

Long, R.M., Singer, R.H., Meng, X., Gonzalez, I., Nasmyth, K., and Jansen, R.P. (1997). Mating type switching in yeast controlled by asymmetric localization of ASH1 mRNA. Science *277*, 383-387.

Markussen, F.H., Michon, A.M., Breitwieser, W., and Ephrussi, A. (1995). Translational control of oskar generates short OSK, the isoform that induces pole plasma assembly. Development *121*, 3723-3732.

Meignin, C., and Davis, I. (2008). UAP56 RNA helicase is required for axis

specification and cytoplasmic mRNA localization in Drosophila. Dev Biol *315*, 89-98.
Minshall, N., and Standart, N. (2004). The active form of Xp54 RNA helicase in translational repression is an RNA-mediated oligomer. Nucleic Acids Res *32*, 1325-1334.
Miyashiro, K., Dichter, M., and Eberwine, J. (1994). On the nature and differential distribution of mRNAs in hippocampal neurites: implications for neuronal functioning. Proc Natl Acad Sci U S A *91*, 10800-10804.
Mlodzik, M., and Gehring, W.J. (1987). Expression of the caudal gene in the germ line of Drosophila: formation of an RNA and protein gradient during early embryogenesis. Cell *48*, 465-478.
Moccia, F., Frost, C., Berra-Romani, R., Tanzi, F., and Adams, D.J. (2004). Expression and function of neuronal nicotinic ACh receptors in rat microvascular endothelial cells. Am J Physiol Heart Circ Physiol *286*, H486-491.
Mohr, S.E., Dillon, S.T., and Boswell, R.E. (2001). The RNA-binding protein Tsunagi interacts with Mago Nashi to establish polarity and localize oskar mRNA during Drosophila oogenesis. Genes Dev *15*, 2886-2899.
Nakamura, A., Amikura, R., Hanyu, K., and Kobayashi, S. (2001). Me31B silences translation of oocyte-localizing RNAs through the formation of cytoplasmic RNP complex during Drosophila oogenesis. Development *128*, 3233-3242.
Nakamura, A., Sato, K., and Hanyu-Nakamura, K. (2004). Drosophila cup is an eIF4E binding protein that associates with Bruno and regulates oskar mRNA translation in oogenesis. Dev Cell *6*, 69-78.
Neuman-Silberberg, F.S., and Schupbach, T. (1993). The Drosophila dorsoventral patterning gene gurken produces a dorsally localized RNA and encodes a TGF alpha-like protein. Cell *75*, 165-174.
Newmark, P.A., and Boswell, R.E. (1994). The mago nashi locus encodes an essential product required for germ plasm assembly in Drosophila. Development *120*, 1303-1313.
Palacios, I.M., Gatfield, D., St Johnston, D., and Izaurralde, E. (2004). An eIF4AIII-containing complex required for mRNA localization and nonsense-mediated mRNA decay. Nature *427*, 753-757.
Palacios, I.M., and St Johnston, D. (2002). Kinesin light chain-independent function of the Kinesin heavy chain in cytoplasmic streaming and posterior localisation in the Drosophila oocyte. Development *129*, 5473-5485.
Parker, R., and Sheth, U. (2007). P bodies and the control of mRNA translation and degradation. Mol Cell *25*, 635-646.
Parker, R., and Song, H. (2004). The enzymes and control of eukaryotic mRNA turnover. Nat Struct Mol Biol *11*, 121-127.

Payre, F., Crozatier, M., and Vincent, A. (1994). Direct control of transcription of the Drosophila morphogen bicoid by the serendipity delta zinc finger protein, as revealed by in vivo analysis of a finger swap. Genes Dev *8*, 2718-2728.

Pokrywka, N.J. (1995). RNA localization and the cytoskeleton in Drosophila oocytes. Curr Top Dev Biol *31*, 139-166.

Reijns, M.A., Alexander, R.D., Spiller, M.P., and Beggs, J.D. (2008). A role for Q/N-rich aggregation-prone regions in P-body localization. J Cell Sci *121*, 2463-2472.

Riechmann, V., and Ephrussi, A. (2001). Axis formation during Drosophila oogenesis. Curr Opin Genet Dev *11*, 374-383.

Riechmann, V., and Ephrussi, A. (2004). Par-1 regulates bicoid mRNA localisation by phosphorylating Exuperantia. Development *131*, 5897-5907.

Rorth, P. (1998). Gal4 in the Drosophila female germline. Mech Dev *78*, 113-118.

Rubin, G.M., and Spradling, A.C. (1982). Genetic transformation of Drosophila with transposable element vectors. Science *218*, 348-353.

Schupbach, T. (1987). Germ line and soma cooperate during oogenesis to establish the dorsoventral pattern of egg shell and embryo in Drosophila melanoga ster. Cell *49*, 699-707.

Sheth, U., and Parker, R. (2003). Decapping and decay of messenger RNA occur in cytoplasmic processing bodies. Science *300*, 805-808.

St Johnston, D. (2005). Moving messages: the intracellular localization of mRNAs. Nat Rev Mol Cell Biol *6*, 363-375.

St Johnston, D., Beuchle, D., and Nusslein-Volhard, C. (1991). Staufen, a gene required to localize maternal RNAs in the Drosophila egg. Cell *66*, 51-63.

Sung, Y.J., Weiler, I.J., Greenough, W.T., and Denman, R.B. (2004). Selectively enriched mRNAs in rat synaptoneurosomes. Brain Res Mol Brain Res *126*, 81-87.

Swan, A., and Suter, B. (1996). Role of Bicaudal-D in patterning the Drosophila egg chamber in mid-oogenesis. Development *122*, 3577-3586.

Takizawa, P.A., Sil, A., Swedlow, J.R., Herskow itz, I., and Vale, R.D. (1997). Actin-dependent localization of an RNA encoding a cell-fate determinant in yeast. Nature *389*, 90-93.

Tange, T.O., Shibuya, T., Jurica, M.S., and Moore, M.J. (2005). Biochemical analysis of the EJC reveals two new factors and a stable tetrameric protein core. RNA *11*, 1869-1883.

Teixeira, D., Sheth, U., Valencia-Sanchez, M.A., Brengues, M., and Parker, R. (2005). Processing bodies require RNA for assembly and contain nontranslating mRNAs. RNA *11*, 371-382.

Theurkauf, W.E., Smiley, S., Wong, M.L., and Alberts, B.M. (1992). Reorganization

of the cytoskeleton during Drosophila oogenesis: implications for axis specification and intercellular transport. Development *115*, 923-936.

Tritschler, F., Eulalio, A., Truffault, V., Hartmann, M. D., Helms, S., Schmidt, S., Coles, M., Izaurralde, E., and Weichenrieder, O. (2007). A divergent Sm fold in EDC3 proteins mediates DCP1 binding and P-body targeting. Mol Cell Biol *27*, 8600-8611.

Tucker, M., and Parker, R. (2000). Mechanisms and control of mRNA decapping in Saccharomyces cerevisiae. Annu Rev Biochem *69*, 571-595.

van Eeden, F.J., Palacios, I.M., Petronczki, M., Weston, M.J., and St Johnston, D. (2001). Barentsz is essential for the posterior localization of oskar mRNA and colocalizes with it to the posterior pole. J Cell Biol *154*, 511-523.

Vanzo, N.F., and Ephrussi, A. (2002). Oskar anchoring restricts pole plasm formation to the posterior of the Drosophila oocyte. Development *129*, 3705-3714.

Wieschaus, E., Nusslein-Volhard, C., and Kluding, H. (1984). Kruppel, a gene whose activity is required early in the zygotic genome for normal embryonic segmentation. Dev Biol *104*, 172-186.

Xu, J., Yang, J.Y., Niu, Q.W., and Chua, N.H. (2006). Arabidopsis DCP2, DCP1, and VARICOSE form a decapping complex required for postembryonic development. Plant Cell *18*, 3386-3398.

Yano, T., Lopez de Quinto, S., Matsui, Y., Shevchenko, A., and Ephrussi, A. (2004). Hrp48, a Drosophila hnRNPA/B homolog, binds and regulates translation of oskar mRNA. Dev Cell *6*, 637-648.

Yao, J., Sasaki, Y., Wen, Z., Bassell, G.J., and Zheng, J.Q. (2006). An essential role for beta-actin mRNA localization and translation in Ca2+-dependent growth cone guidance. Nat Neurosci *9*, 1265-1273.

Yu, J.H., Yang, W.H., Gulick, T., Bloch, K.D., and Bloch, D.B. (2005). Ge-1 is a central component of the mammalian cytoplasmic mRNA processing body. RNA *11*, 1795-1802.

Zhang, J., Houston, D.W., King, M.L., Payne, C., Wylie, C., and Heasman, J. (1998). The role of maternal VegT in establishing the primary germ layers in Xenopus embryos. Cell *94*, 515-524.

Acknowledgments

I am immensely grateful to Anne Ephrussi for giving me the opportunity to pursue my PhD in her lab. Her continuous support, passion for science and the guidance on my projects were really invaluable for me.

I would like to thank the members of my thesis advisory committee, Matthias Hentze, Ed Hurt and Damian Brunner, for their scientific advice and strategic suggestions during my PhD. Many thanks also to Anne Régnier-Vigouroux for agreeing to be a member of my university defense committee and investing the time in reading and evaluating my thesis.

I also would like to acknowledge the following people for the kind sharing of reagents: Tze-Bin Chou for the YFP-dDcp1 flies, Eliza Izaurralde for anti-dGe-1 antibody, and Akira Nakamura for anti-Me31B antibody, anti-Cup antibody, anti-Tral antibody, and the Me31B:EGFP flies.

I also would like to express my appreciation to the former and present members of the Ephrussi lab for their generous help, exciting discussions, as well as friendship, Proteeti Bhattacharjee, Florence Besse, Jean-Baptiste Coutelis, Anna Cyrklaff, Imre Gaspar, Sanjay Ghosh, Ronald Gstir, Helena Jambor, Virginie Marchand, Sandra Müller, Lucas Neidhart, Piyi Papadaki, Sonia Lopez de Quinto, Ritsuko Suyama and Alvar Trucco.

I also would like to express my gratitude to Yen-His Kuo, Helena Jambor, Virginie Marchand for reading and correcting the first draft of my thesis manuscript.

Many thanks to Yawen Chen and Hsin-Ho Sung for helping me begin my life in Germany and for life-long friendship.

Finally, this work is dedicated to my family and Chi-Fang. Without them my life would have been much less enjoyable.